

Background velocity estimation with cross correlations of incoherent waves in the parabolic scaling

Josselin Garnier¹ and Knut Sølna²

¹ Laboratoire de Probabilités et Modèles Aléatoires & Laboratoire Jacques-Louis Lions, Université Paris VII, 2 Place Jussieu, 75251 Paris Cedex 5, France

² Department of Mathematics, University of California, Irvine CA 92697

E-mail: garnier@math.jussieu.fr, ksolna@math.uci.edu

Abstract. In this paper the incoherent waves reflected by a random medium in the parabolic regime are considered. The case in which the medium has three-dimensional rapid random fluctuations and one-dimensional slow variations is analyzed. First, it is shown how the second-order statistics of the reflected wave is determined by the slow spatial variations of the background velocity, the scattering coefficient and the absorption coefficient of the medium via a system of transport equations. Next, it is shown how observations of the intensity, the spatial radius and the spectral radius of the reflected wave, can be used to invert this system in order to reconstruct the parameters of the medium. Finally, it is shown that the analytic framework set forth can also be used to analyze the time dynamics of weak localization.

PACS numbers: 76B15,35Q99,60F05

Submitted to: *Inverse Problems*

1. Introduction

The parabolic regime for wave propagation in random media describes many important physical situations, in geophysics [3], in optics [4, 12], in underwater acoustics [6, 13], or in medical imaging [14]. This regime has been extensively studied and the properties of the transmitted wave are well-known. Much less is known about the reflected waves, because the reflected waves are of small amplitude and incoherent in this regime. However, in many situations (in imaging or remote sensing) only the reflected waves can be measured, and it is therefore important to study them and to show how information about the medium can be extracted from the incoherent reflections. In [8] we showed that the second-order moments of the reflected wave follow a system of transport equations in the case in which the background velocity and impedance are constant, the medium is non-absorbing, and the random fluctuations of the medium are stationary. In this paper we continue this analysis, we now assume that the medium is absorbing and has two types of fluctuations: on the one hand, one-dimensional, deterministic, slow and smooth variations, and on the other hand three-dimensional, random and rapid fluctuations. In this case the heterogeneities in the medium do not create coherent reflected waves, the reflected wave is incoherent. We develop the generalized system of transport equations in this inhomogeneous case, and we show how the second-order statistics of the reflected wave depend on the slow variations of the parameters of the medium. With this result we show that it is possible to image the medium from the observation of the incoherent reflected waves, in the sense that it is possible to invert the system of transport equations from the observation of the cross correlations of the reflected wave and to reconstruct the one-dimensional, slowly varying components of the parameters of the medium.

Inverse problems in which one seeks to detect large scale features of the environment from multiply scattered waves have been addressed in a number of configurations, in particular in [1, 5, 7, 11, 18]. In these papers the authors address the situation in which the slow background variations and the rapid random fluctuations of the medium are one-dimensional. In our paper we discuss the case in which the slow background variations are one-dimensional and the rapid random fluctuations are three-dimensional. This setting is particularly relevant for background velocity estimation in geophysics. The formulation we use here is similar to the one used in [1], the information about the large scale features of the medium is contained in the cross moments of the reflected wave, which are solutions of transport equations in which the background velocity appear. The inverse problem then consists in inverting the system of transport equations.

In addition to solving the inverse problem, the analysis of the second-order statistics of the reflected wave allows us to study carefully the enhanced backscattering phenomenon. Enhanced backscattering (or weak localization) refers to the phenomenon that, when an incoming plane wave is applied with a given incidence angle, the mean reflected power has a local maximum in the backscattered direction, twice as large as

the mean reflected power in the other directions. It was first predicted by physicists [2, 17] and then observed in several experimental contexts [10, 15, 16, 19]. In this paper we study the dynamics of weak localization. We show that the enhanced backscattering factor converges in time to two at an exponential rate, while the angular width of the enhanced backscattering cone decays as a power law.

The paper is organized as follows. We introduce the scaling regime and the quantities of interest in Section 2, and we present the system of transport equations for the reflection operator in Section 3. Then, we study systematically the second-order statistics of the reflected waves, including enhanced backscattering, in Section 4. We use our results in the context of imaging problems in Section 5. Finally, in Section 6, we carry out numerical simulations in the case in which the background velocity or the statistical properties of the microstructure is stepwise constant, and when the detection problem involves identification of the depth of the interface at which the parameters change and also the parameters of the medium on either side.

2. Waves in a random medium

We consider linear acoustic waves propagating in $1 + d$ spatial dimensions with heterogeneous and random medium fluctuations. The governing equations are

$$\rho^\varepsilon(z, \mathbf{x}) \frac{\partial \mathbf{u}^\varepsilon}{\partial t} + \nabla p^\varepsilon + \gamma^\varepsilon(z, \mathbf{x}) \mathbf{u}^\varepsilon = \mathbf{F}^\varepsilon, \quad \frac{1}{K^\varepsilon(z, \mathbf{x})} \frac{\partial p^\varepsilon}{\partial t} + \nabla \cdot \mathbf{u}^\varepsilon = 0, \quad (1)$$

where p^ε is the pressure, \mathbf{u}^ε is the velocity, ρ^ε is the density of the medium, K^ε is the bulk modulus of the medium, γ^ε is the absorption coefficient, and $(z, \mathbf{x}) \in \mathbb{R} \times \mathbb{R}^d$ are the space coordinates. The source is modeled by the forcing term \mathbf{F}^ε . Here we shall focus on propagation through and reflection from a random slab occupying the interval $z \in (0, L)$ with the source \mathbf{F}^ε located outside of the slab, in the half-space $z > L$. The parameterization is motivated by waves probing for instance the heterogeneous earth and one may think of z as the main probing direction. We shall refer to waves propagating in a direction with a positive z component as right-propagating waves.

2.1. Scaling

We consider the parabolic scaling where the medium has one-dimensional, slow and smooth background variations, the ones that we want to identify in the imaging problem, and three-dimensional, small, rapid and random fluctuations. We consider the following model for the bulk modulus K^ε , density ρ^ε , and absorption γ^ε :

$$\frac{1}{K^\varepsilon(z, \mathbf{x})} = \begin{cases} K_0^{-1}(z) & \text{if } z \in (-\infty, 0), \\ K_0^{-1}(z) \left(1 + \varepsilon \nu \left(z, \frac{z}{\varepsilon^2}, \frac{\mathbf{x}}{\varepsilon}\right)\right) & \text{if } z \in (0, L), \\ K_0^{-1}(z) & \text{if } z \in (L, \infty), \end{cases}$$

$$\rho^\varepsilon(z, \mathbf{x}) = \rho_0(z),$$

$$\gamma^\varepsilon(z, \mathbf{x}) = \begin{cases} 0 & \text{if } z \in (-\infty, 0), \\ \gamma_0(z) & \text{if } z \in (0, L), \\ 0 & \text{if } z \in (L, \infty), \end{cases}$$

where ε is a small parameter and K_0 and ρ_0 are smooth functions (of class \mathcal{C}^2). In this scaling regime, the macroscopic scale of variations in the z -direction is one, while the microscopic (and random) scale of variations is of order ε^2 . The amplitude of the random fluctuations is weak, of order ε . The random field $\nu(z, z', \mathbf{x}')$ models the spatial fluctuations of the medium. For a fixed z , we assume that $(z', \mathbf{x}') \mapsto \nu(z, z', \mathbf{x}')$ is a zero-mean stationary random process which satisfies strong mixing conditions with respect to the variable z' . The dependence with respect to the first variable z models a macroscopic, slow variation of the statistical properties of the random fluctuations. As we will see, the important statistical information is contained in the autocorrelation function of the fluctuations of the medium defined by

$$C(z, z', \mathbf{x}') = \mathbb{E}[\nu(z, z'' + z', \mathbf{x}'' + \mathbf{x}')\nu(z, z'', \mathbf{x}'')]. \quad (2)$$

We consider a scaling where the central wavelength of the source is of order ε^2 and write

$$\mathbf{F}^\varepsilon(t, z, \mathbf{x}) = \frac{1}{\varepsilon} f\left(\frac{t}{\varepsilon^2}, \frac{\mathbf{x}}{\varepsilon}\right) \delta(z - z_0) \mathbf{e}_z, \quad (3)$$

with $z_0 > L$, and \mathbf{e}_z the unit vector pointing in the z -direction. The strong amplitude factor $1/\varepsilon$ ensures that the reflected wave has a typical amplitude of order one. Our objective is to characterize the reflected wave, that is, the wave field reflected back from the random slab (at $z = L$).

In order to identify equations that give a convenient description of coupling between different wave modes we now decompose the pressure and longitudinal velocity fields as:

$$p^\varepsilon(t, z, \mathbf{x}) = \frac{\zeta_0(z)^{1/2}}{2\pi} \int \left(\check{a}^\varepsilon\left(\omega, z, \frac{\mathbf{x}}{\varepsilon}\right) e^{i\frac{\omega\tau_0(z)}{\varepsilon^2}} + \check{b}^\varepsilon\left(\omega, z, \frac{\mathbf{x}}{\varepsilon}\right) e^{-i\frac{\omega\tau_0(z)}{\varepsilon^2}} \right) e^{-i\frac{\omega t}{\varepsilon^2}} d\omega, \quad (4)$$

$$\mathbf{e}_z \cdot \mathbf{u}^\varepsilon(t, z, \mathbf{x}) = \frac{\zeta_0(z)^{-1/2}}{2\pi} \int \left(\check{a}^\varepsilon\left(\omega, z, \frac{\mathbf{x}}{\varepsilon}\right) e^{i\frac{\omega\tau_0(z)}{\varepsilon^2}} - \check{b}^\varepsilon\left(\omega, z, \frac{\mathbf{x}}{\varepsilon}\right) e^{-i\frac{\omega\tau_0(z)}{\varepsilon^2}} \right) e^{-i\frac{\omega t}{\varepsilon^2}} d\omega, \quad (5)$$

where \check{a}^ε and \check{b}^ε are generalized right-propagating and left-propagating modes respectively. Here we have introduced the background impedance $\zeta_0(z)$, velocity $c_0(z)$, and travel time $\tau_0(z)$:

$$\zeta_0(z) = \sqrt{K_0(z)\rho_0(z)}, \quad c_0(z) = \frac{\sqrt{K_0(z)}}{\sqrt{\rho_0(z)}}, \quad \tau_0(z) = \int_0^z \frac{dz'}{c_0(z')}.$$

In the homogeneous medium ($\nu = 0$ and ρ_0, K_0, γ_0 independent of z), the expressions (4-5) give a decomposition into uncoupled right- and left-propagating modes [6]. In the inhomogeneous case, by substituting (4-5) into the wave equations (1) we obtain the following coupled mode equations:

$$\begin{aligned} \frac{d\check{a}^\varepsilon}{dz} &= (\mathcal{L}_1^\varepsilon + \mathcal{L}_2^\varepsilon)\check{a}^\varepsilon + e^{-2i\frac{\omega\tau_0(z)}{\varepsilon^2}} (\mathcal{L}_1^\varepsilon + \mathcal{L}_2^\varepsilon)\check{b}^\varepsilon \\ &\quad - \frac{\gamma_0(z)}{2\zeta_0(z)} (\check{a}^\varepsilon - e^{-2i\frac{\omega\tau_0(z)}{\varepsilon^2}} \check{b}^\varepsilon) - \frac{\zeta_0'(z)}{2\zeta_0(z)} e^{-2i\frac{\omega\tau_0(z)}{\varepsilon^2}} \check{b}^\varepsilon, \end{aligned} \quad (6)$$

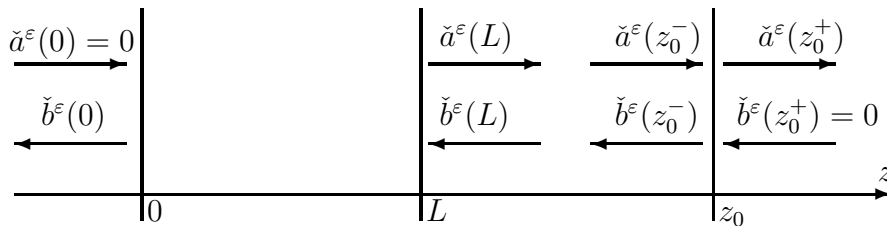


Figure 1. Boundary conditions for the modes in the presence of a random slab $(0, L)$ and a source at $z = z_0$.

$$\begin{aligned} \frac{d\check{b}^\varepsilon}{dz} = & -e^{2i\frac{\omega\tau_0(z)}{\varepsilon^2}}(\mathcal{L}_1^\varepsilon + \mathcal{L}_2^\varepsilon)\check{a}^\varepsilon - (\mathcal{L}_1^\varepsilon + \mathcal{L}_2^\varepsilon)\check{b}^\varepsilon \\ & - \frac{\gamma_0(z)}{2\zeta_0(z)}(e^{2i\frac{\omega\tau_0(z)}{\varepsilon^2}}\check{a}^\varepsilon - \check{b}^\varepsilon) - \frac{\zeta_0'(z)}{2\zeta_0(z)}e^{2i\frac{\omega\tau_0(z)}{\varepsilon^2}}\check{a}^\varepsilon, \end{aligned} \quad (7)$$

where

$$\mathcal{L}_1^\varepsilon = \frac{i\omega}{2c_0(z)\varepsilon}\nu\left(z, \frac{z}{\varepsilon^2}, \mathbf{x}\right), \quad \mathcal{L}_2^\varepsilon = \frac{i}{2\frac{\omega}{c_0(z)} + 2i\varepsilon^2\frac{\gamma_0(z)}{\zeta_0(z)}}\Delta_\perp,$$

Δ_\perp is the transverse Laplacian and ζ_0' is the spatial derivative of ζ_0 . The transverse velocity field $\mathbf{e}_{x_i} \cdot \mathbf{u}^\varepsilon(t, \mathbf{x}, z)$, $i = 1, \dots, d$, can be expressed in terms of the modes \check{a}^ε and \check{b}^ε as

$$\begin{aligned} \mathbf{e}_{x_i} \cdot \mathbf{u}^\varepsilon(t, z, \mathbf{x}) = & \frac{\zeta_0(z)^{-1/2}}{2\pi} \int \frac{-\varepsilon i}{\frac{\omega}{c_0(z)} + i\varepsilon^2\frac{\gamma_0(z)}{\zeta_0(z)}} \left(\frac{\partial \check{a}^\varepsilon}{\partial x_i} \left(\omega, z, \frac{\mathbf{x}}{\varepsilon} \right) e^{i\frac{\omega\tau_0(z)}{\varepsilon^2}} \right. \\ & \left. + \frac{\partial \check{b}^\varepsilon}{\partial x_i} \left(\omega, z, \frac{\mathbf{x}}{\varepsilon} \right) e^{-i\frac{\omega\tau_0(z)}{\varepsilon^2}} \right) e^{-i\frac{\omega t}{\varepsilon^2}} d\omega. \end{aligned}$$

2.2. Boundary conditions

The mode amplitudes \check{a}^ε and \check{b}^ε satisfy the system (6-7) in the random slab $z \in (0, L)$. This system can be complemented with boundary conditions corresponding to the presence of the source term (3) in the plane $z = z_0$, with $z_0 > L$. In the regions $z \in (-\infty, 0)$, $z \in (L, z_0)$ and $z \in (z_0, \infty)$ the medium is slowly varying and non-absorbing. The last terms in (6-7) average to zero as $\varepsilon \rightarrow 0$ due to the fast phases. As a result, the mode amplitudes satisfy the uncoupled paraxial equations

$$\frac{d\check{a}^\varepsilon}{dz} = \frac{ic_0(z)}{2\omega}\Delta_\perp\check{a}^\varepsilon, \quad \frac{d\check{b}^\varepsilon}{dz} = -\frac{ic_0(z)}{2\omega}\Delta_\perp\check{b}^\varepsilon.$$

Taking into account the fact that there is no source in $(-\infty, 0)$, the right-going mode amplitudes \check{a}^ε are zero in this half-space. By the continuity of the fields p^ε and $\mathbf{e}_z \cdot \mathbf{u}^\varepsilon$ at $z = 0$, this gives the first boundary condition

$$\check{a}^\varepsilon(\omega, z = 0, \mathbf{x}) = 0. \quad (8)$$

Taking into account the fact that there is no source in (z_0, ∞) , the left-going mode amplitudes \check{b}^ε are zero in this half-space. The jump conditions across the source

interface $z = z_0$ then give the relation

$$\check{b}^\varepsilon(\omega, z_0^-, \mathbf{x}) = -\frac{1}{2\zeta_0(z_0)^{1/2}\varepsilon} e^{i\frac{\omega\tau_0(z_0)}{\varepsilon^2}} \check{f}(\omega, \mathbf{x}),$$

where the time Fourier transform is defined by

$$\check{f}(\omega, \mathbf{x}) = \int f(t, \mathbf{x}) e^{i\omega t} dt. \quad (9)$$

By solving the paraxial wave equation for \check{b}^ε in the region $z \in (L, z_0)$, we obtain the expression of the complex amplitude of the wave incoming in the random slab at $z = L$:

$$\check{b}^\varepsilon(\omega, L, \mathbf{x}) = \frac{1}{\varepsilon} e^{i\frac{\omega\tau_0(L)}{\varepsilon^2}} \check{b}_{\text{inc}}(\omega, \mathbf{x}), \quad (10)$$

$$\check{b}_{\text{inc}}(\omega, \mathbf{x}) = \frac{-1}{2(2\pi)^d \zeta_0(z_0)^{1/2}} e^{i\frac{\omega[\tau_0(z_0) - \tau_0(L)]}{\varepsilon^2}} \int \hat{f}(\omega, \boldsymbol{\kappa}) e^{-\frac{i}{2\omega} |\boldsymbol{\kappa}|^2 \int_L^{z_0} c_0(z) dz + i\boldsymbol{\kappa} \cdot \mathbf{x}} d\boldsymbol{\kappa}, \quad (11)$$

where the transverse spatial Fourier transform is defined by

$$\hat{f}(\omega, \boldsymbol{\kappa}) = \int \check{f}(\omega, \mathbf{x}) e^{-i\boldsymbol{\kappa} \cdot \mathbf{x}} d\mathbf{x}. \quad (12)$$

In the case in which the source is located just at the exterior of the random slab, $z_0 = L^+$, we simply have

$$\check{b}^\varepsilon(\omega, L, \mathbf{x}) = \frac{1}{\varepsilon} e^{i\frac{\omega\tau_0(L)}{\varepsilon^2}} \check{b}_{\text{inc}}(\omega, \mathbf{x}), \quad \check{b}_{\text{inc}}(\omega, \mathbf{x}) = -\frac{1}{2\zeta_0(L)^{1/2}} \check{f}(\omega, \mathbf{x}). \quad (13)$$

2.3. Multimode wave equations

We shall make use of an invariant imbedding step and introduce reflection and transmission operators. First, we define the transverse Fourier modes

$$\hat{a}^\varepsilon(\omega, z, \boldsymbol{\kappa}) = \int \check{a}^\varepsilon(\omega, z, \mathbf{x}) e^{-i\boldsymbol{\kappa} \cdot \mathbf{x}} d\mathbf{x}, \quad \hat{b}^\varepsilon(\omega, z, \boldsymbol{\kappa}) = \int \check{b}^\varepsilon(\omega, z, \mathbf{x}) e^{-i\boldsymbol{\kappa} \cdot \mathbf{x}} d\mathbf{x}, \quad (14)$$

and make the ansatz

$$\hat{b}^\varepsilon(\omega, 0, \boldsymbol{\kappa}) = \int \hat{\mathcal{T}}^\varepsilon(\omega, z, \boldsymbol{\kappa}, \boldsymbol{\kappa}') \hat{b}^\varepsilon(\omega, z, \boldsymbol{\kappa}') d\boldsymbol{\kappa}', \quad (15)$$

$$\hat{a}^\varepsilon(\omega, z, \boldsymbol{\kappa}) = \int \hat{\mathcal{R}}^\varepsilon(\omega, z, \boldsymbol{\kappa}, \boldsymbol{\kappa}') \hat{b}^\varepsilon(\omega, z, \boldsymbol{\kappa}') d\boldsymbol{\kappa}'. \quad (16)$$

The incoming wave is given by $\hat{b}^\varepsilon(\omega, L, \boldsymbol{\kappa}')$, the operator $\hat{\mathcal{T}}^\varepsilon(\omega, L, \boldsymbol{\kappa}, \boldsymbol{\kappa}')$ maps it to the wave $\hat{b}^\varepsilon(\omega, 0, \boldsymbol{\kappa})$ transmitted to $z = 0$ while the operator $\hat{\mathcal{R}}^\varepsilon(\omega, L, \boldsymbol{\kappa}, \boldsymbol{\kappa}')$ maps it to the wave $\hat{a}^\varepsilon(\omega, L, \boldsymbol{\kappa})$ reflected from the random slab at $z = L$.

Using the mode coupling equations (6-7) one finds

$$\begin{aligned} \frac{d}{dz} \hat{\mathcal{R}}^\varepsilon(\omega, z, \boldsymbol{\kappa}, \boldsymbol{\kappa}') &= e^{-2i\frac{\omega\tau_0(z)}{\varepsilon^2}} \hat{\mathcal{L}}^\varepsilon(\omega, z, \boldsymbol{\kappa}, \boldsymbol{\kappa}') \\ &+ e^{2i\frac{\omega\tau_0(z)}{\varepsilon^2}} \iint \hat{\mathcal{R}}^\varepsilon(\omega, z, \boldsymbol{\kappa}, \boldsymbol{\kappa}_1) \hat{\mathcal{L}}^\varepsilon(\omega, z, \boldsymbol{\kappa}_1, \boldsymbol{\kappa}_2) \hat{\mathcal{R}}^\varepsilon(\omega, z, \boldsymbol{\kappa}_2, \boldsymbol{\kappa}') d\boldsymbol{\kappa}_1 d\boldsymbol{\kappa}_2 \\ &+ \int \hat{\mathcal{L}}^\varepsilon(\omega, z, \boldsymbol{\kappa}, \boldsymbol{\kappa}_1) \hat{\mathcal{R}}^\varepsilon(\omega, z, \boldsymbol{\kappa}_1, \boldsymbol{\kappa}') + \hat{\mathcal{R}}^\varepsilon(\omega, z, \boldsymbol{\kappa}, \boldsymbol{\kappa}_1) \hat{\mathcal{L}}^\varepsilon(\omega, z, \boldsymbol{\kappa}_1, \boldsymbol{\kappa}') d\boldsymbol{\kappa}_1 \end{aligned} \quad (17)$$

$$\begin{aligned}
& + \left(\frac{\gamma_0(z)}{2\zeta_0(z)} + \frac{\zeta'_0(z)}{2\zeta_0(z)} \right) e^{2i\frac{\omega\tau_0(z)}{\varepsilon^2}} \int \hat{\mathcal{R}}^\varepsilon(\omega, z, \boldsymbol{\kappa}, \boldsymbol{\kappa}_1) \hat{\mathcal{R}}^\varepsilon(\omega, z, \boldsymbol{\kappa}_1, \boldsymbol{\kappa}') d\boldsymbol{\kappa}_1 \\
& - \frac{\gamma_0(z)}{\zeta_0(z)} \hat{\mathcal{R}}^\varepsilon(\omega, z, \boldsymbol{\kappa}, \boldsymbol{\kappa}') + \left(\frac{\gamma_0(z)}{\zeta_0(z)} + \frac{\zeta'_0(z)}{2\zeta_0(z)} \right) e^{-2i\frac{\omega\tau_0(z)}{\varepsilon^2}} \delta(\boldsymbol{\kappa} - \boldsymbol{\kappa}'), \\
\frac{d}{dz} \hat{\mathcal{T}}^\varepsilon(\omega, z, \boldsymbol{\kappa}, \boldsymbol{\kappa}') & = \int \hat{\mathcal{T}}^\varepsilon(\omega, z, \boldsymbol{\kappa}, \boldsymbol{\kappa}_1) \hat{\mathcal{L}}^\varepsilon(\omega, z, \boldsymbol{\kappa}_1, \boldsymbol{\kappa}') d\boldsymbol{\kappa}_1 \\
& + e^{2i\frac{\omega\tau_0(z)}{\varepsilon^2}} \iint \hat{\mathcal{T}}^\varepsilon(\omega, z, \boldsymbol{\kappa}, \boldsymbol{\kappa}_1) \hat{\mathcal{L}}^\varepsilon(\omega, z, \boldsymbol{\kappa}_1, \boldsymbol{\kappa}_2) \hat{\mathcal{R}}^\varepsilon(\omega, z, \boldsymbol{\kappa}_2, \boldsymbol{\kappa}') d\boldsymbol{\kappa}_1 d\boldsymbol{\kappa}_2 \\
& + \left(\frac{\gamma_0(z)}{2\zeta_0(z)} + \frac{\zeta'_0(z)}{2\zeta_0(z)} \right) e^{2i\frac{\omega\tau_0(z)}{\varepsilon^2}} \int \hat{\mathcal{T}}^\varepsilon(\omega, z, \boldsymbol{\kappa}, \boldsymbol{\kappa}_1) \hat{\mathcal{R}}^\varepsilon(\omega, z, \boldsymbol{\kappa}_1, \boldsymbol{\kappa}') d\boldsymbol{\kappa}_1 \\
& + \frac{\gamma_0(z)}{2\zeta_0(z)} \hat{\mathcal{T}}^\varepsilon(\omega, z, \boldsymbol{\kappa}, \boldsymbol{\kappa}'),
\end{aligned} \tag{18}$$

where we have defined

$$\hat{\mathcal{L}}^\varepsilon(\omega, z, \boldsymbol{\kappa}_1, \boldsymbol{\kappa}_2) = - \frac{i|\boldsymbol{\kappa}_1|^2}{2\frac{\omega}{c_0(z)} + 2i\varepsilon^2\frac{\gamma_0(z)}{\zeta_0(z)}} \delta(\boldsymbol{\kappa}_1 - \boldsymbol{\kappa}_2) + \frac{i\omega}{\varepsilon 2(2\pi)^d c_0(z)} \hat{\nu}\left(z, \frac{z}{\varepsilon^2}, \boldsymbol{\kappa}_1 - \boldsymbol{\kappa}_2\right), \tag{19}$$

with $\hat{\nu}(z, \boldsymbol{\kappa})$ the partial Fourier transform of $\nu(z, \mathbf{x})$ as defined by (12). This system is supplemented with the initial conditions

$$\hat{\mathcal{R}}^\varepsilon(\omega, z = 0, \boldsymbol{\kappa}, \boldsymbol{\kappa}') = 0, \quad \hat{\mathcal{T}}^\varepsilon(\omega, z = 0, \boldsymbol{\kappa}, \boldsymbol{\kappa}') = \delta(\boldsymbol{\kappa} - \boldsymbol{\kappa}'), \tag{20}$$

corresponding to the boundary condition (8) and the fact that the medium is matched there. The reflected wave field observed at the surface $z = L$ and at the scale \mathbf{x}/ε is

$$\begin{aligned}
p_{\text{ref}}^\varepsilon(t, \mathbf{x}) & = \frac{\zeta_0(L)^{1/2}}{2\pi} \int \check{a}^\varepsilon(\omega, L, \mathbf{x}) e^{i\frac{\omega\tau_0(L)}{\varepsilon^2}} e^{-i\frac{\omega t}{\varepsilon^2}} d\omega \\
& = \frac{\zeta_0(L)^{1/2}}{(2\pi)^{d+1}\varepsilon} \iint \int \hat{\mathcal{R}}^\varepsilon(\omega, L, \boldsymbol{\kappa}, \boldsymbol{\kappa}') \hat{b}_{\text{inc}}(\omega, \boldsymbol{\kappa}') e^{i\boldsymbol{\kappa} \cdot \mathbf{x}} e^{i\frac{\omega}{\varepsilon^2}[2\tau_0(L) - t]} d\omega d\boldsymbol{\kappa} d\boldsymbol{\kappa}'.
\end{aligned}$$

3. Asymptotic analysis of the reflection operator

3.1. Transport equations in the weak backscattering regime

The reflection operator $\hat{\mathcal{R}}^\varepsilon$ solves (17) with the initial condition (20). Proposition A.1 in Appendix A shows that it is possible to compute the cross moments of the reflection operator using diffusion approximation theory in the limit $\varepsilon \rightarrow 0$. The set of transport equations (58) describes the statistics of the reflected wave. However, the system is rather complicated and the corresponding inverse problem would not be easy to solve. In this subsection we introduce a simplified system which holds when random backscattering is weaker than random forward scattering.

In the following we assume that the spectrum of the source is contained in $\pm[\omega_0(1 - B), \omega_0(1 + B)]$ where ω_0 is the carrier frequency and $2B$ is the relative bandwidth. A central quantity that characterizes the backscattered wave field is the cross spectral density

$$W_{(\boldsymbol{\kappa}_1, \boldsymbol{\kappa}_2), (\boldsymbol{\kappa}_3, \boldsymbol{\kappa}_4)}(\omega, \tau, z)$$

$$= \lim_{\varepsilon \rightarrow 0} \frac{1}{2\pi} \int \mathbb{E} \left[\widehat{\mathcal{R}}^\varepsilon \left(\omega + \frac{\varepsilon^2 h}{2}, z, \boldsymbol{\kappa}_1, \boldsymbol{\kappa}_2 \right) \overline{\widehat{\mathcal{R}}^\varepsilon \left(\omega - \frac{\varepsilon^2 h}{2}, z, \boldsymbol{\kappa}_3, \boldsymbol{\kappa}_4 \right)} \right] e^{-ih[\tau - 2\tau_0(z)]} dh. \quad (21)$$

This quantity describes the cross correlations of the reflected wave field

$$\begin{aligned} \lim_{\varepsilon \rightarrow 0} \mathbb{E} [p_{\text{ref}}^\varepsilon(t, \mathbf{x}) p_{\text{ref}}^\varepsilon(t + \varepsilon^2 s, \mathbf{x}')] &= \frac{\zeta_0(L)}{(2\pi)^{2d+1}} \int \cdots \int W_{(\boldsymbol{\kappa}_1, \boldsymbol{\kappa}_2), (\boldsymbol{\kappa}_3, \boldsymbol{\kappa}_4)}(\omega, t, L) \\ &\times e^{i\boldsymbol{\kappa}_1 \cdot \mathbf{x} - i\boldsymbol{\kappa}_3 \cdot \mathbf{x}'} e^{i\omega s} \widehat{b}_{\text{inc}}(\omega, \boldsymbol{\kappa}_2) \overline{\widehat{b}_{\text{inc}}(\omega, \boldsymbol{\kappa}_4)} d\omega d\boldsymbol{\kappa}_1 d\boldsymbol{\kappa}_2 d\boldsymbol{\kappa}_3 d\boldsymbol{\kappa}_4. \end{aligned} \quad (22)$$

We are interested in this quantity in the regime of weak backscattering. This regime derives from the modeling assumption

$$\delta := \sup_{\boldsymbol{\kappa} \in \mathbb{R}^d, z \in (0, L), \omega \in [\omega_0(1-B), \omega_0(1+B)]} \frac{\widehat{C}(z, 2\omega/c_0(z), \boldsymbol{\kappa})}{\widehat{C}(z, 0, \mathbf{0})} \ll 1, \quad (23)$$

where \widehat{C} is the Fourier transform of the autocorrelation function C defined by

$$\widehat{C}(z, k, \boldsymbol{\kappa}) = \int_{\mathbb{R}^d} \int_{-\infty}^{\infty} C(z, z', \mathbf{x}') e^{-i(kz' + \boldsymbol{\kappa} \cdot \mathbf{x}')} dz' d\mathbf{x}'. \quad (24)$$

As can be seen in Appendix A, the term $\widehat{C}(z, 2\omega/c_0(z), \boldsymbol{\kappa})$ is proportional to the conversion rate (at depth z) between right- and left- going modes, while $\widehat{C}(z, 0, \boldsymbol{\kappa})$ is proportional to the conversion rate between two left-going modes (or between two right-going modes).

Proposition 3.1 *In the weak backscattering regime the cross spectral density $W_{(\boldsymbol{\kappa}_1, \boldsymbol{\kappa}_2), (\boldsymbol{\kappa}_3, \boldsymbol{\kappa}_4)}(\omega, \tau, z)$ defined by (21) has the form*

$$W_{(\boldsymbol{\kappa}_1, \boldsymbol{\kappa}_2), (\boldsymbol{\kappa}_3, \boldsymbol{\kappa}_4)}(\omega, \tau, z) = V_{\boldsymbol{\kappa}_2 - \boldsymbol{\kappa}_4, \boldsymbol{\kappa}_1 + \boldsymbol{\kappa}_4, \boldsymbol{\kappa}_1 - \boldsymbol{\kappa}_2}(\omega, \tau, z) \delta(\boldsymbol{\kappa}_1 - \boldsymbol{\kappa}_2 - \boldsymbol{\kappa}_3 + \boldsymbol{\kappa}_4), \quad (25)$$

where $V_{\boldsymbol{\kappa}_u, \boldsymbol{\kappa}_v, \boldsymbol{\kappa}_w}(\omega, \tau, z)$ is the solution of the system of transport equations

$$\begin{aligned} \frac{\partial V_{\boldsymbol{\kappa}_u, \boldsymbol{\kappa}_v, \boldsymbol{\kappa}_w}}{\partial z} + \frac{2}{c_0(z)} \frac{\partial V_{\boldsymbol{\kappa}_u, \boldsymbol{\kappa}_v, \boldsymbol{\kappa}_w}}{\partial \tau} &= -\frac{2\gamma_0(z)}{\zeta_0(z)} V_{\boldsymbol{\kappa}_u, \boldsymbol{\kappa}_v, \boldsymbol{\kappa}_w} - \frac{ic_0(z)}{\omega} \boldsymbol{\kappa}_u \cdot \boldsymbol{\kappa}_v V_{\boldsymbol{\kappa}_u, \boldsymbol{\kappa}_v, \boldsymbol{\kappa}_w} \\ &+ \frac{\omega^2}{4(2\pi)^d c_0^2(z)} \int \widehat{C}(z, 0, \boldsymbol{\kappa}) \left\{ V_{\boldsymbol{\kappa}_u, \boldsymbol{\kappa}_v - \boldsymbol{\kappa}, \boldsymbol{\kappa}_w - \boldsymbol{\kappa}} + V_{\boldsymbol{\kappa}_u, \boldsymbol{\kappa}_v - \boldsymbol{\kappa}, \boldsymbol{\kappa}_w + \boldsymbol{\kappa}} + V_{\boldsymbol{\kappa}_u - \boldsymbol{\kappa}, \boldsymbol{\kappa}_v, \boldsymbol{\kappa}_w - \boldsymbol{\kappa}} \right. \\ &\quad \left. + V_{\boldsymbol{\kappa}_u - \boldsymbol{\kappa}, \boldsymbol{\kappa}_v, \boldsymbol{\kappa}_w + \boldsymbol{\kappa}} - V_{\boldsymbol{\kappa}_u - \boldsymbol{\kappa}, \boldsymbol{\kappa}_v - \boldsymbol{\kappa}, \boldsymbol{\kappa}_w} - V_{\boldsymbol{\kappa}_u + \boldsymbol{\kappa}, \boldsymbol{\kappa}_v - \boldsymbol{\kappa}, \boldsymbol{\kappa}_w} - 2V_{\boldsymbol{\kappa}_u, \boldsymbol{\kappa}_v, \boldsymbol{\kappa}_w} \right\} d\boldsymbol{\kappa} \\ &+ \frac{\omega^2}{4(2\pi)^d c_0^2(z)} \widehat{C}\left(z, \frac{2\omega}{c_0(z)}, \boldsymbol{\kappa}_w\right) \delta(\tau), \end{aligned} \quad (26)$$

starting from $V_{\boldsymbol{\kappa}_u, \boldsymbol{\kappa}_v, \boldsymbol{\kappa}_w}(\omega, \tau, z = 0) = 0$.

This proposition is proved in Appendix A and it shows that the second-order statistics of the reflected wave depends on the large features of the medium through the system of transport equations (26). The inverse problem consists in determining the coefficients of the transport equations from the solution V . In fact, we will see in the following that we do not need to know all of V in order to solve the inverse problem, because of the one-dimensional structure of the large features of the medium.

Note that the density V is symmetric in $(\boldsymbol{\kappa}_u, \boldsymbol{\kappa}_v)$: $V_{\boldsymbol{\kappa}_u, \boldsymbol{\kappa}_v, \boldsymbol{\kappa}_w}(\omega, \tau, z) = V_{\boldsymbol{\kappa}_v, \boldsymbol{\kappa}_u, \boldsymbol{\kappa}_w}(\omega, \tau, z)$. This can be seen from the structure of the system (26), and this also follows directly from the reciprocity relation $\widehat{\mathcal{R}}^\varepsilon(\boldsymbol{\kappa}, \boldsymbol{\kappa}') = \widehat{\mathcal{R}}^\varepsilon(-\boldsymbol{\kappa}', -\boldsymbol{\kappa})$.

3.2. Mean reflected intensity

As a first application, we compute the mean reflected intensity at time t :

$$I^\varepsilon(t) = \frac{1}{\zeta_0(L)} \int \mathbb{E}[p_{\text{ref}}^\varepsilon(t, \mathbf{x})^2] d\mathbf{x}. \quad (27)$$

Proposition 3.2 *The mean reflected intensity $I^\varepsilon(t)$ has the limit $I(t)$ as $\varepsilon \rightarrow 0$:*

$$I(t) = \frac{1}{(2\pi)^{d+1}} \int P_{\text{ref}}(\omega, t) \left[\int |\hat{b}_{\text{inc}}(\omega, \boldsymbol{\kappa}')|^2 d\boldsymbol{\kappa}' \right] d\omega, \quad (28)$$

where

$$P_{\text{ref}}(\omega, t) = \frac{\omega^2}{8c_0(z(t))} \check{C} \left(z(t), \frac{2\omega}{c_0(z(t))}, \mathbf{0} \right) e^{-2 \int_{z(t)}^L \frac{\gamma_0(z')}{\zeta_0(z')} dz'}. \quad (29)$$

Here \check{C} is the partial Fourier transform of the autocorrelation function C

$$\check{C}(z, k, \mathbf{x}) = \int C(z, z', \mathbf{x}) e^{-ikz'} dz', \quad (30)$$

and $z(t) \in (0, L)$ is such that

$$\int_{z(t)}^L \frac{1}{c_0(z')} dz' = \frac{t}{2}. \quad (31)$$

This proposition is proved in Appendix C. Remember that the total input energy is

$$E_{\text{inc}} = \frac{1}{(2\pi)^{d+1}} \iint |\hat{b}_{\text{inc}}(\omega, \boldsymbol{\kappa}')|^2 d\boldsymbol{\kappa}' d\omega, \quad (32)$$

so that $P_{\text{ref}}(\omega, t)$ can be interpreted as the spectral density of reflected power at time t . Note that $P(\omega, t)$ and $I(t)$ are zero if $t \notin (0, 2\tau_0(L))$. The distance $z(t)$ corresponds to a round trip from L to $z(t)$ whose duration is t when moving with the background velocity $c_0(z)$. In the expression (29) the term $\frac{\omega^2}{8c_0(z)} \check{C}(z, \frac{2\omega}{c_0(z)}, \mathbf{0})$ gives the generation rate of backpropagating waves at depth z and $\exp(-2 \int_z^L \frac{\gamma_0(z')}{\zeta_0(z')} dz')$ is the damping due to a round trip from L to z in the absorbing medium.

If the background velocity c_0 , impedance ζ_0 , absorption γ_0 and the function \check{C} do not depend on z , then the mean reflected intensity is zero if $t \notin (0, 2L/c_0)$. If $t \in (0, 2L/c_0)$, then we have $z(t) = L - c_0 t/2$ and

$$P_{\text{ref}}(\omega, t) = \frac{\omega^2}{8c_0} \check{C} \left(\frac{2\omega}{c_0}, \mathbf{0} \right) e^{-c_0 t \frac{\gamma_0}{\zeta_0}},$$

which shows that the reflected intensity decays exponentially in time due to absorption.

4. The second-order statistics of the reflected wave

It is possible to get closed-form expressions for physically relevant quantities from the system (26). These expressions become especially simple in a special regime that we

now describe. From now on we assume that the random fluctuations of the medium are smooth so that the autocorrelation function C is at least twice differentiable at $\mathbf{x} = \mathbf{0}$:

$$\Delta_{\mathbf{x}}C(z, 0, \mathbf{0}) = -\frac{1}{(2\pi)^{d+1}} \iint |\boldsymbol{\kappa}|^2 \widehat{C}(z, k, \boldsymbol{\kappa}) dk d\boldsymbol{\kappa} < 0.$$

The longitudinal (respectively transverse) correlation radius l_z (resp. l_x) of the random fluctuations and the standard deviation σ of the fluctuations can be defined as follows:

$$\begin{aligned} \sigma^2 &= \frac{1}{L} \int_0^L C(z, 0, \mathbf{0}) dz, \\ \sigma^2 l_z &= \frac{1}{L} \int_0^L \int C(z, z', \mathbf{0}) dz' dz, \\ \frac{\sigma^2}{l_x^2} &= -\frac{1}{dL} \int_0^L \Delta_{\mathbf{x}}C(z, 0, \mathbf{0}) dz. \end{aligned}$$

Note that it is possible to adopt other definitions for these quantities, as we will only use their orders of magnitudes in this paper. If we also introduce the typical speed of sound \bar{c} of the medium, then the parameters

$$\alpha = \frac{\bar{c}L}{\omega_0 l_x^2}, \quad \beta = \frac{\omega_0^2 L \sigma^2 l_z}{4\bar{c}^2}, \quad (33)$$

are the two dimensionless parameters that determine the behavior of the cross spectral density, as is shown in Appendix B. For a given propagation distance L , the parameter α is the inverse of the Fresnel number for the transverse scale l_x , and it characterizes the strength of diffraction at this scale, while the parameter β characterizes the strength of random forward scattering. The strength of random backscattering relative to random forward scattering is δ defined by (23).

In Appendix D we analyze the behavior of the cross spectral density in the limit case $\alpha \rightarrow \infty$. This result allows us to get closed-form expressions for the physically relevant quantities. We consider the time-resolved reflected beam width in Subsection 4.1, the spectral width in Subsection 4.2, the spatial and spectral cross correlation functions in Subsections 4.3-4.4. We study the dynamics of enhanced backscattering in Subsection 4.5.

4.1. Beam width

We define the rms (root-mean-squared) width $R^\varepsilon(t)$ of the reflected wave at time t by

$$R^{\varepsilon 2}(t) = \frac{\int |\mathbf{x}|^2 \mathbb{E}[p_{\text{ref}}^\varepsilon(t, \mathbf{x})^2] d\mathbf{x}}{\int \mathbb{E}[p_{\text{ref}}^\varepsilon(t, \mathbf{x})^2] d\mathbf{x}}. \quad (34)$$

Proposition 4.1 *The beam width $R^\varepsilon(t)$ converges to $R(t)$ as $\varepsilon \rightarrow 0$, where $R(t)$ is given by*

$$R^2(t) = R_0^2 - \frac{1}{2} \int_{z(t)}^L c_0^{-2}(z') \Delta_{\mathbf{x}} \check{C}(z', 0, \mathbf{0}) \left[\left(\int_{z(t)}^L c_0(z'') dz'' \right)^2 + \left(\int_{z(t)}^{z'} c_0(z'') dz'' \right)^2 \right] dz'$$

$$\begin{aligned}
& + 4 \frac{K_0^2}{\omega_0^2} \left(\int_{z(t)}^L c_0(z') dz' \right)^2 + 4 \frac{Q_0}{\omega_0} \left(\int_{z(t)}^L c_0(z') dz' \right) \\
& - \frac{1}{\omega_0^2} \frac{\Delta_{\mathbf{x}} \check{C}(z(t), \frac{2\omega_0}{c_0(z(t))}, \mathbf{0})}{\check{C}(z(t), \frac{2\omega_0}{c_0(z(t))}, \mathbf{0})} \left(\int_{z(t)}^L c_0(z') dz' \right)^2, \tag{35}
\end{aligned}$$

in the regime where $\alpha \gg 1$ and the relative bandwidth $B \ll 1$. Here $z(t)$ is defined by (31), R_0 (respectively K_0) is the rms beam width (respectively spectral width) of the input beam:

$$R_0^2 = \frac{\iint |\mathbf{x}|^2 |\hat{b}_{\text{inc}}(\omega, \mathbf{x})|^2 d\mathbf{x} d\omega}{\iint |\hat{b}_{\text{inc}}(\omega, \mathbf{x})|^2 d\mathbf{x} d\omega}, \quad K_0^2 = \frac{\iint |\boldsymbol{\kappa}|^2 |\hat{b}_{\text{inc}}(\omega, \boldsymbol{\kappa})|^2 d\boldsymbol{\kappa} d\omega}{\iint |\hat{b}_{\text{inc}}(\omega, \boldsymbol{\kappa})|^2 d\boldsymbol{\kappa} d\omega}, \tag{36}$$

and Q_0 is defined by

$$Q_0 = \frac{\iint \boldsymbol{\kappa} \cdot \text{Im} \left(\hat{b}_{\text{inc}} \overline{\nabla_{\boldsymbol{\kappa}} \hat{b}_{\text{inc}}}(\omega, \boldsymbol{\kappa}) \right) d\boldsymbol{\kappa} d\omega}{\iint |\hat{b}_{\text{inc}}(\omega, \boldsymbol{\kappa})|^2 d\boldsymbol{\kappa} d\omega} = \frac{-\iint \mathbf{x} \cdot \text{Im} \left(\hat{b}_{\text{inc}} \overline{\nabla_{\mathbf{x}} \hat{b}_{\text{inc}}}(\omega, \mathbf{x}) \right) d\mathbf{x} d\omega}{\iint |\hat{b}_{\text{inc}}(\omega, \mathbf{x})|^2 d\mathbf{x} d\omega}. \tag{37}$$

This proposition is proved in Appendix E. For instance, in the case of a narrowband Gaussian beam $b_{\text{inc}}(t, \mathbf{x})$ with a spatial chirp, obtained by sending a Gaussian beam with radius r_0 through a converging ($b_0 < 0$) or diverging ($b_0 > 0$) lens, we have:

$$\hat{b}_{\text{inc}}(\omega, \boldsymbol{\kappa}) = \hat{g}(\omega) e^{-\frac{1}{2}(1+i\frac{b_0}{\omega})r_0^2|\boldsymbol{\kappa}|^2}, \quad R_0^2 = \frac{r_0^2}{2} \left(1 + \frac{b_0^2}{\omega_0^2} \right), \quad K_0^2 = \frac{1}{2r_0^2}, \quad Q_0 = \frac{b_0}{2\omega_0}, \tag{38}$$

with \hat{g} the Fourier transform of the pulse function of the source with carrier frequency ω_0 .

We can interpret all terms in the expression (35):

- (i) The first term (with R_0) is the initial beam width.
- (ii) The second term (with $\Delta_{\mathbf{x}} \check{C}(z', 0, \mathbf{0})$) is the spreading effect due to random forward scattering; it is the only term (with the initial beam width) that is independent of ω_0 (i.e., of the frequency).
- (iii) The third term (with K_0) is due to the natural beam diffraction.
- (iv) The fourth term (with Q_0) is a convergence of divergence effect due to the curvature of the initial beam phase front; this term is the only one in the sum that can be negative; the condition $Q_0 < 0$ means that the input beam has an initial phase front that makes it converge, but this convergence is eventually overwhelmed by natural diffraction, and also by the spreading induced by random scattering.
- (v) The last term (with $\Delta_{\mathbf{x}} \check{C}(z(t), \frac{2\omega_0}{c_0}, \mathbf{0})$) is the spreading induced by random backward scattering. This term is pointwise, in the sense that it depends only on the properties of the medium at $z(t)$, while the forward scattering term (ii) is cumulative and depends on the properties of the medium between $z(t)$ and L .

If the background velocity c_0 and the function \check{C} do not depend on z , then the squared rms radius has a cubic polynomial expression in terms of $t \in (0, 2L/c_0)$:

$$R^2(t) = R_0^2 - \frac{2}{3} \Delta_{\mathbf{x}} \check{C}(0, \mathbf{0}) \left(\frac{c_0 t}{2} \right)^3 + 4 \frac{K_0^2 c_0^2}{\omega_0^2} \left(\frac{c_0 t}{2} \right)^2$$

$$+ 4 \frac{Q_0 c_0}{\omega_0} \left(\frac{c_0 t}{2} \right) - \frac{c_0^2}{\omega_0^2} \frac{\Delta_{\mathbf{x}} \check{C}(\frac{2\omega_0}{c_0}, \mathbf{0})}{\check{C}(\frac{2\omega_0}{c_0}, \mathbf{0})} \left(\frac{c_0 t}{2} \right)^2. \quad (39)$$

This shows that the random forward scattering is the dominant phenomenon for long times and that the beam width increases like $t^{3/2}$.

4.2. Spectral width

We define the rms spectral width $K^\varepsilon(t)$ of the reflected wave at time t by

$$K^{\varepsilon 2}(t) = \frac{\int \mathbb{E}[|\nabla_{\mathbf{x}} p_{\text{ref}}^\varepsilon(t, \mathbf{x})|^2] d\mathbf{x}}{\int \mathbb{E}[p_{\text{ref}}^\varepsilon(t, \mathbf{x})^2] d\mathbf{x}} = \frac{\int |\boldsymbol{\kappa}|^2 \mathbb{E}[|\hat{p}_{\text{ref}}^\varepsilon(t, \boldsymbol{\kappa})|^2] d\boldsymbol{\kappa}}{\int \mathbb{E}[|\hat{p}_{\text{ref}}^\varepsilon(t, \boldsymbol{\kappa})|^2] d\boldsymbol{\kappa}}. \quad (40)$$

Proposition 4.2 *The spectral width $K^\varepsilon(t)$ converges to $K(t)$ as $\varepsilon \rightarrow 0$, where $K(t)$ is given by*

$$K^2(t) = K_0^2 - \frac{\omega_0^2}{2} \int_{z(t)}^L c_0^{-2}(z') \Delta_{\mathbf{x}} \check{C}(z', 0, \mathbf{0}) dz' - \frac{\Delta_{\mathbf{x}} \check{C}(z(t), \frac{2\omega_0}{c_0(z(t))}, \mathbf{0})}{\check{C}(z(t), \frac{2\omega_0}{c_0(z(t))}, \mathbf{0})}, \quad (41)$$

in the regime $\alpha \gg 1$.

This proposition is proved in Appendix F. In the expression (41),

- (i) the first term K_0^2 is the initial spectral width (squared),
- (ii) the second term (with $\Delta_{\mathbf{x}} \check{C}(z', 0, \mathbf{0})$) is the spectral broadening due to random forward scattering during the round trip from L to $z(t)$,
- (iii) the third term is the spectral broadening due to random backward scattering at $z(t)$.

If the background velocity c_0 and the function \check{C} do not depend on z , then the squared rms spectral width has a linear expression in terms of $t \in (0, 2L/c_0)$:

$$K^2(t) = K_0^2 - \frac{\omega_0^2}{2c_0^2} \Delta_{\mathbf{x}} \check{C}(0, \mathbf{0}) \left(\frac{c_0 t}{2} \right) - \frac{\Delta_{\mathbf{x}} \check{C}(\frac{2\omega_0}{c_0}, \mathbf{0})}{\check{C}(\frac{2\omega_0}{c_0}, \mathbf{0})}. \quad (42)$$

This shows that the spectral broadening is dominated by the random forward scattering for long times and that the spectral width grows like $t^{1/2}$.

4.3. Spatial cross correlation function

Here we consider the spatial cross correlation function:

$$A^\varepsilon(t, \mathbf{x}) = \frac{\int \mathbb{E}[p_{\text{ref}}^\varepsilon(t, \mathbf{x}') p_{\text{ref}}^\varepsilon(t, \mathbf{x}' + \mathbf{x})] d\mathbf{x}'}{\int \mathbb{E}[p_{\text{ref}}^\varepsilon(t, \mathbf{x}')^2] d\mathbf{x}'}$$

Proposition 4.3 *The spatial cross correlation function $A^\varepsilon(t, \mathbf{x})$ has the limit $A(t, \mathbf{x})$ as $\varepsilon \rightarrow 0$, where $A(t, \mathbf{x})$ is given by*

$$A(t, \mathbf{x}) = \frac{\check{C}(z(t), \frac{2\omega_0}{c_0(z(t))}, \mathbf{x})}{\check{C}(z(t), \frac{2\omega_0}{c_0(z(t))}, \mathbf{0})} e^{\frac{\omega_0^2}{2} \int_{z(t)}^L c_0^{-2}(z') [\check{C}(z', 0, \mathbf{x}) - \check{C}(z', 0, \mathbf{0})] dz'} \frac{\iint e^{-i\boldsymbol{\kappa}' \cdot \mathbf{x}} |\hat{b}_{\text{inc}}(\omega, \boldsymbol{\kappa}')|^2 d\boldsymbol{\kappa}' d\omega}{\iint |\hat{b}_{\text{inc}}(\omega, \boldsymbol{\kappa}')|^2 d\boldsymbol{\kappa}' d\omega}, \quad (43)$$

in the regime where $\alpha \gg 1$ and the relative bandwidth $B \ll 1$.

This proposition is proved in Appendix G. There are three contributions in the spatial cross correlation function (43):

- (i) The first term is the contribution of the random backscattering at $z(t)$.
- (ii) The second term is the contribution of random forward scattering during the round trip from L to $z(t)$.
- (iii) The third term is the contribution of the spatial diversity of the input beam. It is negligible if the transverse correlation length l_x of the random fluctuations of the medium is smaller than the beam width R_0 .

If the background velocity c_0 and the function \check{C} do not depend on z , then we have for any $t \in (0, 2L/c_0)$:

$$A(t, \mathbf{x}) = \frac{\check{C}\left(\frac{2\omega_0}{c_0}, \mathbf{x}\right)}{\check{C}\left(\frac{2\omega_0}{c_0}, \mathbf{0}\right)} e^{\frac{\omega_0^2}{2c_0^2} [\check{C}(0, \mathbf{x}) - \check{C}(0, \mathbf{0})] \left(\frac{c_0 t}{2}\right)} \frac{\iint e^{-i\boldsymbol{\kappa}' \cdot \mathbf{x}} |\hat{b}_{\text{inc}}(\omega, \boldsymbol{\kappa}')|^2 d\boldsymbol{\kappa}' d\omega}{\iint |\hat{b}_{\text{inc}}(\omega, \boldsymbol{\kappa}')|^2 d\boldsymbol{\kappa}' d\omega}.$$

This shows that, for small times, the cross correlation function is determined by the form of the input beam and the spatial distribution of the backscattering process. For times large enough so that $\beta(c_0 t)/L \gg 1$, the form of the cross correlation function is determined by the random forward scattering and we have approximately, if \check{C} is isotropic in \mathbf{x} :

$$A(t, \mathbf{x}) \stackrel{\beta(c_0 t)/L \gg 1}{\simeq} e^{\frac{\omega_0^2 t}{4c_0 d} \Delta_{\mathbf{x}} \check{C}(0, \mathbf{0}) |\mathbf{x}|^2},$$

which shows that correlation radius decays as $t^{-1/2}$.

4.4. Spectral cross correlation function

Here we consider the spectral cross correlation function:

$$S^\varepsilon(t, \boldsymbol{\kappa}) = \frac{\int \mathbb{E}[\hat{p}_{\text{ref}}^\varepsilon(t, \boldsymbol{\kappa}') \overline{\hat{p}_{\text{ref}}^\varepsilon(t, \boldsymbol{\kappa}' + \boldsymbol{\kappa})}] d\boldsymbol{\kappa}'}{\int \mathbb{E}[|\hat{p}_{\text{ref}}^\varepsilon(t, \boldsymbol{\kappa}')|^2] d\boldsymbol{\kappa}'}$$

Proposition 4.4 *The spectral cross correlation function $S^\varepsilon(t, \boldsymbol{\kappa})$ has the limit $S(t, \boldsymbol{\kappa})$ as $\varepsilon \rightarrow 0$, where $S(t, \boldsymbol{\kappa})$ is given by*

$$\begin{aligned} S(t, \boldsymbol{\kappa}) &= \frac{\check{C}\left(z(t), \frac{2\omega_0}{c_0(z(t))}, \frac{J_0(L) - J_0(z(t))}{\omega_0} \boldsymbol{\kappa}\right)}{\check{C}\left(z(t), \frac{2\omega_0}{c_0(z(t))}, \mathbf{0}\right)} \\ &\times e^{\frac{\omega_0^2}{4} \int_{z(t)}^L c_0^{-2}(z') \left\{ \check{C}\left(z', 0, [J_0(L) - 2J_0(z(t)) + J_0(z')] \frac{\boldsymbol{\kappa}}{\omega_0}\right) + \check{C}\left(z', 0, [J_0(L) - J_0(z')] \frac{\boldsymbol{\kappa}}{\omega_0}\right) - 2\check{C}\left(z', 0, \mathbf{0}\right) \right\} dz'} \\ &\times \frac{\iint e^{2i[J_0(L) - J_0(z(t))] \frac{\boldsymbol{\kappa} \cdot \boldsymbol{\kappa}_2}{\omega_0}} |\hat{b}_{\text{inc}}(\omega, \boldsymbol{\kappa}_2)|^2 d\boldsymbol{\kappa}_2 d\omega}{\iint |\hat{b}_{\text{inc}}(\omega, \boldsymbol{\kappa}_2)|^2 d\boldsymbol{\kappa}_2 d\omega}, \end{aligned} \quad (44)$$

in the regime where $\alpha \gg 1$ and the relative bandwidth $B \ll 1$. Here $z(t)$ is defined by (31) and

$$J_0(z) = \int_0^z c_0(z') dz'. \quad (45)$$

This proposition is proved in Appendix H. If the background velocity c_0 and the function \check{C} do not depend on z , then we have for any $t \in (0, 2L/c_0)$:

$$S(t, \boldsymbol{\kappa}) = \frac{\check{C}\left(\frac{2\omega_0}{c_0}, \frac{c_0 t}{2} \frac{c_0 \boldsymbol{\kappa}}{\omega_0}\right)}{\check{C}\left(\frac{2\omega_0}{c_0}, \mathbf{0}\right)} e^{\frac{\omega_0^2}{4c_0^2} \int_0^{c_0 t} \{\check{C}(0, z') - \check{C}(0, 0)\} dz'} \frac{\iint e^{ic_0 t \frac{c_0 \boldsymbol{\kappa} \cdot \boldsymbol{\kappa}_2}{\omega_0}} |\hat{b}_{\text{inc}}(\omega, \boldsymbol{\kappa}_2)|^2 d\boldsymbol{\kappa}_2 d\omega}{\iint |\hat{b}_{\text{inc}}(\omega, \boldsymbol{\kappa}_2)|^2 d\boldsymbol{\kappa}_2 d\omega}.$$

If $\beta \ll 1$ (i.e. if random forward scattering is weak), then the form of the spectral cross correlation function is determined by the input beam and the backscattering process. If $\beta \gg 1$, then the form of the cross correlation function is determined by random forward scattering and we have approximately, if \check{C} is isotropic in \mathbf{x} :

$$S(t, \boldsymbol{\kappa}) \stackrel{\beta \gg 1}{\simeq} e^{\frac{c_0^3 t^3}{24d} \Delta_{\mathbf{x}} \check{C}(0, \mathbf{0})} |\boldsymbol{\kappa}|^2,$$

which shows that the spectral coherence radius decays as $t^{-3/2}$.

4.5. Enhanced backscattering

In this section, we study the dynamics of enhanced backscattering, and compute the time dependence of the maximum, the angular width, and the shape of the enhanced backscattering cone.

We consider the following experiment: for a given $\boldsymbol{\kappa}_0$, we send a quasi-plane wave with carrier frequency ω_0 , carrier wavevector $\boldsymbol{\kappa}_0$, and angular aperture much smaller than $\alpha^{-1}(\omega_0 l_x / \bar{c})^{-1}$. We record the reflected power in the backscattered direction $-\boldsymbol{\kappa}_0$ or close to it, in a cone of angular aperture of order $\alpha^{-1}(\omega_0 l_x / \bar{c})^{-1}$. Accordingly we observe

$$\begin{aligned} |\hat{p}_{\text{ref}}^\varepsilon(t, -\boldsymbol{\kappa}_0 + \boldsymbol{\kappa})|^2 &= \left| \int p_{\text{ref}}^\varepsilon(t, \mathbf{x}) e^{-i(-\boldsymbol{\kappa}_0 + \boldsymbol{\kappa}) \cdot \mathbf{x}} d\mathbf{x} \right|^2 \\ &= \frac{\zeta_0(L)}{(2\pi)^{2\varepsilon}} \left| \iint \hat{\mathcal{R}}^\varepsilon(\omega, L, -\boldsymbol{\kappa}_0 + \boldsymbol{\kappa}, \boldsymbol{\kappa}') e^{i\frac{\omega}{\varepsilon^2} [2\tau_0(L) - t]} \hat{b}_{\text{inc}}(\omega, \boldsymbol{\kappa}') d\boldsymbol{\kappa}' d\omega \right|^2. \end{aligned}$$

If we perform a series of such experiments with different incoming directions and average with respect to the incoming direction, then we observe, in the asymptotic regime $\varepsilon \rightarrow 0$,

$$P_{\boldsymbol{\kappa}}(t) = \lim_{\varepsilon \rightarrow 0} \frac{1}{(2\pi)^d \zeta_0(L)} \int \mathbb{E}[|\hat{p}_{\text{ref}}^\varepsilon(t, -\boldsymbol{\kappa}_0 + \boldsymbol{\kappa})|^2] d\boldsymbol{\kappa}_0.$$

Proposition 4.5 *The mean reflected power observed in the relative direction $\boldsymbol{\kappa}$ (relatively to the backscattered direction) is*

$$\begin{aligned} P_{\boldsymbol{\kappa}}(t) &= P_\infty(t) \left[1 - e^{-\frac{\omega_0^2}{2} \int_{z(t)}^L c_0^{-2}(z') \check{C}(z', \mathbf{0}, \mathbf{0}) dz'} \right. \\ &\quad \left. + e^{\frac{\omega_0^2}{2} \int_{z(t)}^L c_0^{-2}(z') \left\{ \check{C}(z', 0, [J_0(L) - J_0(z')] \frac{\boldsymbol{\kappa}}{\omega_0}) - \check{C}(z', \mathbf{0}, \mathbf{0}) \right\} dz'} \right], \end{aligned} \quad (46)$$

in the regime $\alpha \gg 1$. Here $z(t)$ is defined by (31),

$$P_\infty(t) = \frac{\pi^d E_{\text{inc}} \omega_0^2}{8c_0(z(t))} \check{C}\left(z(t), \frac{2\omega_0}{c_0(z(t))}, \mathbf{0}\right) e^{-2 \int_{z(t)}^L \frac{\gamma_0(z')}{\zeta_0(z')} dz'}, \quad (47)$$

and E_{inc} is given by (32).

This proposition is proved in Appendix I. The reflected intensity $P_{\boldsymbol{\kappa}}(t)$ goes from $P_{\infty}(t)$ for $\frac{cL}{\omega_0 l_x} |\boldsymbol{\kappa}| \gg 1$ to the maximal value $P_{\infty}(t) f_{\text{EBC}}(t)$ reached for $\boldsymbol{\kappa} = \mathbf{0}$, where the enhancement factor is

$$f_{\text{EBC}}(t) = 2 - e^{-\frac{\omega_0^2}{2} \int_{z(t)}^L c_0^{-2}(z') \check{C}(z', \mathbf{0}, \mathbf{0}) dz'}.$$

If the background velocity c_0 and the function \check{C} do not depend on z , then we have for any $t \in (0, 2L/c_0)$:

$$f_{\text{EBC}}(t) = 2 - e^{-\frac{\omega_0^2}{4c_0} \check{C}(\mathbf{0}, \mathbf{0}) t},$$

which shows that the enhancement factor goes from 1 to $2 - \exp(-\check{C}(\mathbf{0}, \mathbf{0}) \frac{\omega_0^2 L}{2c_0^2})$ (close to 2 if $\beta \gg 1$) at an exponential rate in time. The shape of the cone is

$$P_{\boldsymbol{\kappa}}(t) = P_{\infty}(t) \left[1 - e^{-\frac{\omega_0^2}{4c_0} \check{C}(\mathbf{0}, \mathbf{0}) t} + e^{\frac{\omega_0^2}{2c_0^2} \int_0^{c_0 t/2} \{ \check{C}(0, c_0 z' \frac{\boldsymbol{\kappa}}{\omega_0}) - \check{C}(\mathbf{0}, \mathbf{0}) \} dz'} \right].$$

If random forward scattering is strong ($\beta \gg 1$) and \check{C} is isotropic in \mathbf{x} , then for t large enough so that $\beta(c_0 t/L) \gg 1$, we have

$$P_{\boldsymbol{\kappa}}(t) \simeq P_{\infty}(t) \left[1 + e^{\frac{c_0^3 t^3}{96d} \Delta_{\mathbf{x}} \check{C}(\mathbf{0}, \mathbf{0}) |\boldsymbol{\kappa}|^2} \right],$$

which shows that the width of the cone decays as $t^{-3/2}$. Note that:

- (i) The asymptotic Gaussian shape of the cone is obtained if the random fluctuations of the medium are smooth so that the autocorrelation function is twice differentiable at $\mathbf{x} = \mathbf{0}$. If the fluctuations are rough, then the cone has a cusp at $\boldsymbol{\kappa} = \mathbf{0}$ [8].
- (ii) The angular width of the cone is proportional to the wavelength, as predicted by the physical theory based on diagrammatic expansions [17].

5. Statistical stability and inverse problems

5.1. Preliminary discussion

Here we discuss the conditions under which the second-order statistics of the reflected field can be observed. The formula (22) gives in particular

$$\lim_{\varepsilon \rightarrow 0} \frac{\int \mathbb{E}[p_{\text{ref}}^{\varepsilon}(t, \mathbf{x}) p_{\text{ref}}^{\varepsilon}(t + \varepsilon^2 s, \mathbf{x})] d\mathbf{x}}{\int \mathbb{E}[p_{\text{ref}}^{\varepsilon}(t, \mathbf{x})^2] d\mathbf{x}} = \frac{\int P_{\text{ref}}(\omega, t) e^{i\omega s} \left[\int |\hat{b}_{\text{inc}}(\omega, \boldsymbol{\kappa}')|^2 d\boldsymbol{\kappa}' \right] d\omega}{\int P_{\text{ref}}(\omega, t) \left[\int |\hat{b}_{\text{inc}}(\omega, \boldsymbol{\kappa}')|^2 d\boldsymbol{\kappa}' \right] d\omega},$$

which goes to zero when $s \rightarrow \infty$ by Riemann-Lebesgue lemma. This shows that the coherence time of the reflected wave is of order ε^2 . Therefore, we can claim that, for any $p \in (0, 2)$, we have

$$\lim_{\varepsilon \rightarrow 0} \frac{1}{2\varepsilon^p} \int_{t-\varepsilon^p}^{t+\varepsilon^p} p_{\text{ref}}^{\varepsilon}(t', \mathbf{x}) p_{\text{ref}}^{\varepsilon}(t', \mathbf{x}') dt' = \lim_{\varepsilon \rightarrow 0} \mathbb{E}[p_{\text{ref}}^{\varepsilon}(t, \mathbf{x}) p_{\text{ref}}^{\varepsilon}(t, \mathbf{x}')].$$

A rigorous approach would make use of the fourth-order moments. This involves the study of $W_{\mathbf{p},\mathbf{q}}$ for $n_{\mathbf{p}} = n_{\mathbf{q}} = 2$ (defined in the Appendix A), which is beyond the scope of this paper.

The power delay spread (i.e. the duration of the reflected wave) is of the order of $2L/\bar{c}$, while the coherence time is of the order of the initial pulse width ε^2 . By time-windowing the reflected wave into time-intervals long compared to the coherence time, but short compared to the power delay spread, one can get statistically stable estimates of the reflected intensity $I(t)$, the reflected beam width $R(t)$ and the spectral width $K(t)$. From these quantities, one can reconstruct the background velocity $c_0(z)$ and the scattering coefficient $s(z)$

$$s^2(z) = -\Delta_{\mathbf{x}}\check{C}(z, 0, \mathbf{0}),$$

as we show in the next subsection.

5.2. Reconstruction of the background velocity

The identification of the background velocity is an important problem, in geophysics for instance [3]. In the cases in which no strong interface is present, only the analysis of the incoherent reflected wave (as we carry out in this paper) can give an answer to this problem. We next describe how the background velocity can be extracted from the incoherent reflections. By performing two experiments with two input Gaussian chirped beams of the form (38) with different chirps $b_{0,1}$ and $b_{0,2}$ (which affect R_0 and Q_0 , but not K_0), we can observe the differences between the reflected beam widths:

$$\delta_1(t) = \frac{\omega_0^2}{2} \frac{R^2(t, b_{0,2}) - R^2(t, b_{0,1}) - R_0^2(b_{0,2}) + R_0^2(b_{0,1})}{b_{0,2} - b_{0,1}} \stackrel{\text{in theory}}{=} \int_{z(t)}^L c_0(z') dz'. \quad (48)$$

Using the fact that $\frac{dz}{dt} = -\frac{1}{2}c_0(z(t))$, we can compute $z(t)$ by integrating

$$\frac{dz(t)}{dt} = -\sqrt{\frac{1}{2} \frac{d\delta_1(t)}{dt}}, \quad z(0) = L,$$

from which we can get the background velocity by the identity

$$c_0(z(t)) = \sqrt{2 \frac{d\delta_1(t)}{dt}}.$$

Alternatively, by performing two experiments with two input beams with zero chirp and with different carrier frequencies $\omega_{0,1}$ and $\omega_{0,2}$, we can extract from the reflected beam widths:

$$\delta_2(t) = R^2(t, \omega_{0,2}) - R^2(t, \omega_{0,1}),$$

and from the reflected spectral widths:

$$\delta_3(t) = \frac{K^2(t, \omega_{0,2}) + 3K_0^2}{\omega_{0,2}^2} - \frac{K^2(t, \omega_{0,1}) + 3K_0^2}{\omega_{0,1}^2}.$$

Since we have

$$\tilde{\delta}_1(t) = \sqrt{\frac{\delta_2(t)}{\delta_3(t)}} \stackrel{\text{in theory}}{=} \int_{z(t)}^L c_0(z') dz',$$

we can use this result to extract the background velocity from $\tilde{\delta}_1(t)$ as described above with $\delta_1(t)$.

Beyond the background velocity, it is possible to extract the scattering coefficient by observing the spectral widths for two input beams with two different carrier frequencies $\omega_{0,1}$ and $\omega_{0,2}$:

$$\delta_4(t) = 2 \frac{K^2(t, \omega_{0,2}) - K^2(t, \omega_{0,1})}{\omega_{0,2}^2 - \omega_{0,1}^2} \stackrel{\text{in theory}}{=} \int_{z(t)}^L c_0^{-2}(z') s^2(z') dz'.$$

We can get the scattering coefficient $s^2(z)$ by the relation

$$s^2(z(t)) = 2\sqrt{2} \sqrt{\frac{d\delta_1(t)}{dt} \frac{d\delta_4(t)}{dt}}.$$

5.3. Detection of an interface

In this subsection, we consider the situation in which the medium in $(0, L)$ is made of two materials. The slab $(L - z_i, L)$ close to the surface has constant background parameters c_0, ζ_0, γ_0 , and stationary random fluctuations $\check{C}(z, k, \mathbf{x}) = \check{C}_0(k, \mathbf{x})$, as well as the slab $(0, L - z_i)$ whose background parameters and autocorrelation function are denoted by c_1, ζ_1, γ_1 , and $\check{C}(z, k, \mathbf{x}) = \check{C}_1(k, \mathbf{x})$. By sending a narrowband beam and by observing the reflected wave, we aim to extract the parameters $c_j, \gamma_j/\zeta_j$, and $s_j = -\Delta\check{C}_j(0, \mathbf{x})$, $j = 0, 1$, as well as the interface location z_i .

The mean reflected intensity decays exponentially with time, but two exponential branches can be distinguished. More precisely,

$$I(t) = \begin{cases} \frac{\omega_0^2}{8c_0} \check{C}_0\left(\frac{2\omega_0}{c_0}, \mathbf{0}\right) e^{-\frac{c_0\gamma_0}{\zeta_0} t} & \text{if } t < t_i, \\ \frac{\omega_0^2}{8c_1} \check{C}_1\left(\frac{2\omega_0}{c_1}, \mathbf{0}\right) e^{-\frac{c_0\gamma_0}{\zeta_0} t_i} e^{-\frac{c_1\gamma_1}{\zeta_1} \tilde{t}} & \text{if } t_i < t < t_i + 2\frac{L-z_i}{c_1}, \end{cases} \quad (49)$$

where $\tilde{t} = t - t_i$ and

$$t_i = 2\frac{z_i}{c_0}. \quad (50)$$

This shows that there is a jump in the mean reflected intensity at time t_i with the jump amplitude given by

$$\Delta I = \frac{\omega_0^2}{8} \left(\frac{1}{c_1} \check{C}_1\left(\frac{2\omega_0}{c_1}, \mathbf{0}\right) - \frac{1}{c_0} \check{C}_0\left(\frac{2\omega_0}{c_0}, \mathbf{0}\right) \right) e^{-\frac{c_0\gamma_0}{\zeta_0} t_i}.$$

The spectral radius for $t < t_i$ is given by (42) and for $t_i < t < t_i + 2\frac{L-z_i}{c_1}$ by

$$K^2(t) = K_0^2 - \frac{\omega_0^2 t_i}{4c_0} \Delta_{\mathbf{x}} \check{C}_0(0, \mathbf{0}) - \frac{\omega_0^2 \tilde{t}}{4c_1} \Delta_{\mathbf{x}} \check{C}_1(0, \mathbf{0}) - \frac{\Delta_{\mathbf{x}} \check{C}_1\left(\frac{2\omega_0}{c_1}, \mathbf{0}\right)}{\check{C}_1\left(\frac{2\omega_0}{c_1}, \mathbf{0}\right)},$$

where $\tilde{t} = t - t_i$. This shows that $K^2(t)$ is a piecewise-linear function, with a jump at time t_i whose amplitude is given by

$$\Delta K^2 = \frac{\Delta_{\mathbf{x}}\check{C}_0(\frac{2\omega_0}{c_0}, \mathbf{0})}{\check{C}_0(\frac{2\omega_0}{c_0}, \mathbf{0})} - \frac{\Delta_{\mathbf{x}}\check{C}_1(\frac{2\omega_0}{c_1}, \mathbf{0})}{\check{C}_1(\frac{2\omega_0}{c_1}, \mathbf{0})}.$$

The mean squared radius $R^2(t)$ is a piecewise-cubic function. For $t < t_i$ is given by (39) and for $t_i < t < t_i + 2\frac{L-z_i}{c_1}$ by:

$$\begin{aligned} R^2(t) = R_0^2 - & \left[\Delta_{\mathbf{x}}\check{C}_0(0, \mathbf{0}) \left(\frac{1}{8} \left(\frac{c_1^2 \tilde{t}}{c_0} \right)^2 (c_0 t_i) + \frac{3}{16} \left(\frac{c_1^2 \tilde{t}}{c_0} \right) (c_0 t_i)^2 + \frac{1}{12} (c_0 t_i)^3 \right) \right. \\ & \left. + \Delta_{\mathbf{x}}\check{C}_1(0, \mathbf{0}) \left(\frac{1}{12} (c_1 \tilde{t})^3 + \frac{1}{8} \left(\frac{c_0^2 t_i}{c_1} \right) (c_1 \tilde{t})^2 + \frac{1}{16} \left(\frac{c_0^2 t_i}{c_1} \right)^2 (c_1 \tilde{t}) \right) \right] \\ & + \frac{K_0^2}{\omega_0^2} (c_1^2 \tilde{t} + c_0^2 t_i)^2 + 2 \frac{Q_0}{\omega_0} (c_1^2 \tilde{t} + c_0^2 t_i) - \frac{1}{4\omega_0^2} \frac{\Delta_{\mathbf{x}}\check{C}_1(\frac{2\omega_0}{c_1}, \mathbf{0})}{\check{C}_1(\frac{2\omega_0}{c_1}, \mathbf{0})} (c_1^2 \tilde{t} + c_0^2 t_i)^2, \end{aligned} \quad (51)$$

where $\tilde{t} = t - t_i$. There is a jump of the beam radius at time t_i whose amplitude is given by

$$\Delta R^2 = \frac{c_0^4 t_i^2}{4\omega_0^2} \left(\frac{\Delta_{\mathbf{x}}\check{C}_0(\frac{2\omega_0}{c_0}, \mathbf{0})}{\check{C}_0(\frac{2\omega_0}{c_0}, \mathbf{0})} - \frac{\Delta_{\mathbf{x}}\check{C}_1(\frac{2\omega_0}{c_1}, \mathbf{0})}{\check{C}_1(\frac{2\omega_0}{c_1}, \mathbf{0})} \right).$$

We conclude that by measuring the jump time t_i and the jump amplitudes ΔR^2 and ΔK^2 for the beam radius and the spectral radius, we can extract the location of the interface

$$z_i = \sqrt[4]{\frac{\omega_0^2 t_i^2}{4} \frac{\Delta R^2}{\Delta K^2}}.$$

Then, by using the value of t_i we get the background velocity c_0 :

$$c_0 = \frac{z_i}{t_i}.$$

From the slope of $K^2(t)$ for $t < t_i$ we get the scattering coefficient s_0 :

$$s_0^2 = \frac{4c_0}{\omega_0^2} \frac{dK^2(t)}{dt}, \text{ for } 0 < t < t_i.$$

Finally, by using the reflected intensity $I(t)$ for times $t < t_i$ we get the relative absorption parameter γ_0/ζ_0 :

$$\frac{\gamma_0}{\zeta_0} = -\frac{1}{c_0} \frac{d \ln I(t)}{dt}, \text{ for } 0 < t < t_i.$$

This completes the characterization of the parameters in the slab ($L - z_i, L$).

Next, by using the reflected intensity for times $t > t_i$ we get $c_1 \gamma_1/\zeta_1$:

$$\frac{c_1 \gamma_1}{\zeta_1} = -\frac{d \ln I(t)}{dt}, \text{ for } t_i < t < t_i + 2\frac{L - z_i}{c_1}.$$

In order to get c_1 , it is necessary to use two different input beams, either with two different chirps or with two different carrier frequencies. For instance, by performing

two experiments with two input Gaussian chirped beams of the form (38) with different chirps $b_{0,1}$ and $b_{0,2}$, we can observe the differences between the reflected beam widths after time t_i :

$$\delta_1(t) = \frac{\omega_0^2}{2} \frac{R^2(t, b_{0,2}) - R^2(t, b_{0,1}) - R_0^2(b_{0,2}) + R_0^2(b_{0,1})}{b_{0,2} - b_{0,1}} \stackrel{\text{in theory}}{=} c_1^2 \tilde{t} + c_0^2 t_i.$$

Therefore it is a linear function whose slope gives c_1 :

$$c_1 = \sqrt{\frac{d\delta_1}{dt}}, \text{ for } t_i < t < t_i + 2\frac{L - z_i}{c_1}.$$

With c_1 and $c_1\gamma_1/\zeta_1$, we get the absorption coefficient γ_1/ζ_1 . Finally, the slope of $K^2(t)$ after time t_i gives the scattering coefficient

$$s_1^2 = \frac{4c_1}{\omega_0^2} \frac{dK^2(t)}{dt}, \text{ for } t_i < t < t_i + 2\frac{L - z_i}{c_1}.$$

6. Numerical simulations

In this section we assume that there is no background impedance variation and no absorption, and we then wish to extract the background velocity $c_0(z)$ from the measurements of the incoherent reflected waves. Observe that with no impedance contrast there will indeed be no strong interface in the medium generating a coherent reflected wave. The resolution of the full wave equation with several different scales is computationally expensive. Therefore the numerical simulations in a 1 + 1-dimensional space are performed using the iterative scheme proposed in [9]. This scheme allows us to obtain the complex amplitudes $\check{a}(\omega, z, x)$ and $\check{b}(\omega, z, x)$ with a computational cost equivalent to the paraxial wave equation, but with comparable results to the full Helmholtz equation. The algorithm is as follows:

Step 0: start from $\check{a}_0(\omega, z, x) = 0$ for all z .

Step n : solve the paraxial wave equation with source from $z = L$ to $z = 0$:

$$\frac{\partial \check{b}_n}{\partial z} = -\frac{i\omega}{2c_0(z)} \nu(z, x) \check{b}_n - \frac{ic_0(z)}{2\omega} \Delta_{\perp} \check{b}_n - e^{2i\omega\tau_0(z)} \frac{i\omega}{2c_0(z)} \nu(z, x) \check{a}_{n-1},$$

starting from $\check{b}_n(\omega, z = L, x) = \check{b}_{\text{inc}}(\omega, x)$, and then solve the paraxial wave equation with source from $z = 0$ to $z = L$:

$$\frac{\partial \check{a}_n}{\partial z} = \frac{i\omega}{2c_0(z)} \nu(z, x) \check{a}_n + \frac{ic_0(z)}{2\omega} \Delta_{\perp} \check{a}_n + e^{-2i\omega\tau_0(z)} \frac{i\omega}{2c_0(z)} \nu(z, x) \check{b}_n,$$

starting from $\check{a}_n(\omega, z = 0, x) = 0$. We use a split-step Fourier method for solving the random paraxial wave equations (while a finite-difference scheme was used in [9]). Although no convergence theory is (yet) available for this scheme, it has been shown to converge to the solution of the full wave equation by comparison with numerical simulations based on the Helmholtz equation. Moreover, we have observed that the scheme converges very quickly (after two or three steps) in the weak backscattering regime, even when random forward scattering is strong. This scheme is perfectly adapted to our setting.

6.1. Detection of background velocity change

In the first set of numerical simulations the medium consists of two different slabs with the same statistics for the random fluctuations and different background velocities:

$$c_0(z) = \begin{cases} c_0 & \text{for } z \in [L - z_i, L], \\ c_1 & \text{for } z \in [0, L - z_i], \end{cases}$$

with $L = 128$, $z_i = 64$, $c_0 = 1$, and $c_1 = 0.7$. The random process $\nu(z, x)$ has the form

$$\nu(z, x) = \sum_{j=0}^{\infty} \mathbf{1}_{[L_j, L_{j+1})}(z) \nu_j(x),$$

where $L_0 = 0$, $L_j = \sum_{i=1}^j l_i$; l_i are independent and identically distributed random variables with exponential distribution and mean $l_z = 4$; $\nu_j(x)$ are independent and identically distributed Gaussian processes with Gaussian autocorrelation function, standard deviation σ (with $\sigma = 0.01$ or $\sigma = 0.04$), and transverse correlation length $l_x = 10$. We then have

$$\check{C}_{2k}(x) = \check{C}_0(0) \frac{1}{1 + 4k^2 l_z^2} \exp\left(-\frac{x^2}{l_x^2}\right), \quad \check{C}_0(0) = 2\sigma^2 l_z.$$

It follows that with the choice $k_0 = 1$ and $l_z = 4$, we have $\check{C}_{2k_0}(0)/\check{C}_0(0) \simeq 0.016$ which shows that we are indeed in the weak backscattering regime. The incoming beam has a Gaussian shape in space with radius $r_0 = 16$ and a sinc shape in time with a central frequency $\omega_0 = 1$ and a bandwidth $B = 0.15$:

$$b_{\text{inc}}(t, x) = \text{sinc}(Bt) e^{-i\omega_0 t} \exp\left(-\frac{x^2}{2r_0^2}\right) + cc. \quad (52)$$

The separation of scales is not large in our numerical setup due to computational limitations. As a consequence:

- 1) the spatial resolution of the inversion method (which is of the order of the pulse width times the background velocity) is here not very high.
- 2) the statistical stability property is not achieved and one needs to average over a series of independent experiments (here we average over 1000 experiments). In practice, this corresponds to repeating the experiments by moving the source to different (lateral) locations in order to probe different (quasi-independent) regions, while the one-dimensional background velocity profile is constant.

The medium is probed with two different incoming beams with two different chirp parameters $b_{0,1} = 0$ and $b_{0,2} = -2.5$, thus with the latter corresponding passage through a converging lens. The reflected signals are recorded (Figure 2), in particular the reflected powers $I(t, b_{0,1})$ and $I(t, b_{0,2})$ (Figure 3) and the reflected beam widths $R(t, b_{0,1})$ and $R(t, b_{0,2})$ (Figure 4). It can be checked that the reflected power does not depend on the chirp, while the reflected beam width depends on it. The difference (48) is the quantity that is used to determine the background velocity:

$$\delta_1^{(\text{exp})}(t) = \frac{\omega_0^2}{2} \frac{R^2(t, b_{0,2}) - R^2(t, b_{0,1})}{b_{0,2} - b_{0,1}} - \frac{r_0^2}{4} (b_{0,2} + b_{0,1}),$$

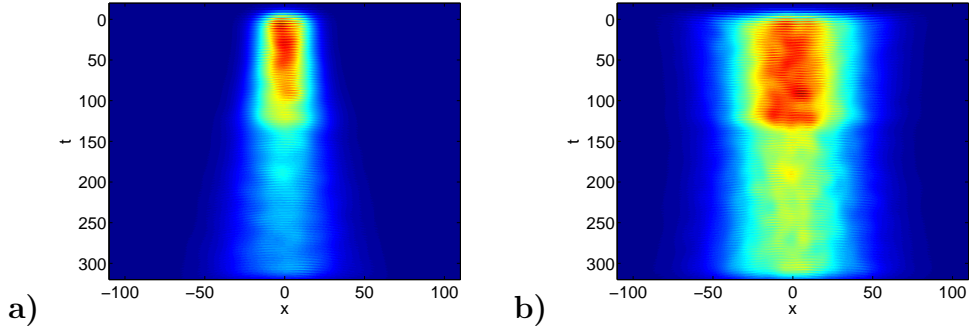


Figure 2. Reflected signals received with the unchirped incoming beam $b_{0,1} = 0$ (a) and the chirped incoming beam $b_{0,2} = -2.5$ (b). In both cases $\sigma = 0.04$.

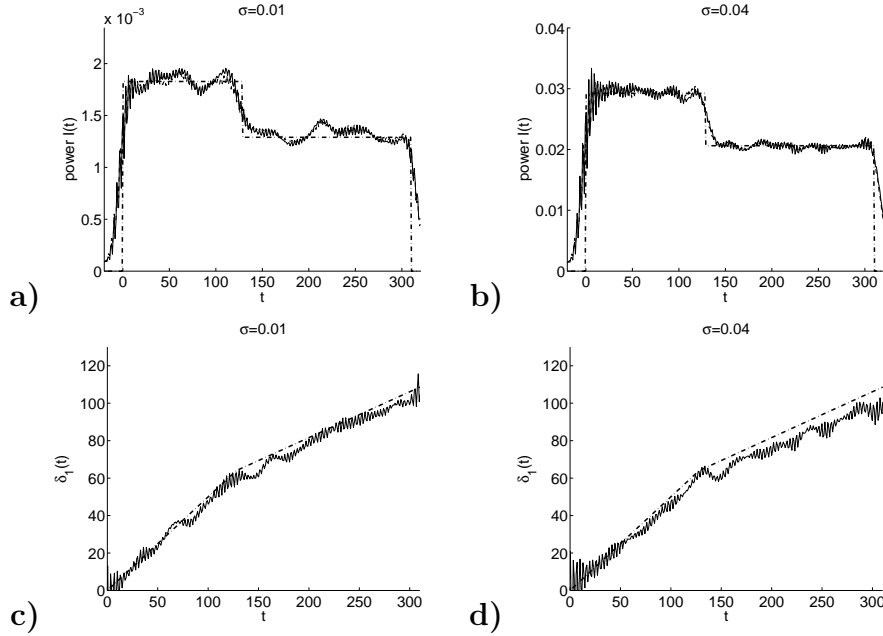


Figure 3. Picture (a): the mean reflected power $I(t)$ for the unchirped and chirped incoming beams (the two thin lines are almost undistinguishable) for $\sigma = 0.01$. The thick dashed line is the theoretical value (49). Picture (b): the mean reflected power $I(t)$ for $\sigma = 0.04$. Picture (c): the difference $\delta_1(t)$ for $\sigma = 0.01$. The thin solid lines are the numerical results and the thick dashed line the theoretical formula (53). Picture (d): the difference $\delta_1(t)$ for $\sigma = 0.04$.

and it is plotted in Figure 3. By a least-square fit of the data $\delta_1^{(\text{exp})}(t)$ with respect to the theoretical formula:

$$\delta_1^{(\text{theo})}(t) = \begin{cases} \frac{c_0^2 t}{2} & \text{for } t < t_i, \\ \frac{c_0^2 t_i}{2} + \frac{c_1^2 (t - t_i)}{2} & \text{for } t_i < t < T, \end{cases} \quad (53)$$

with $t_i = 2z_i/c_a$ and $T = 2z_i/c_0 + 2(L - z_i)/c_1$, we obtain the following estimates of the quantities c_0 , c_1 , t_i , and z_i (the theoretical values are $c_0 = 1$, $c_1 = 0.7$, $t_i = 128$, and

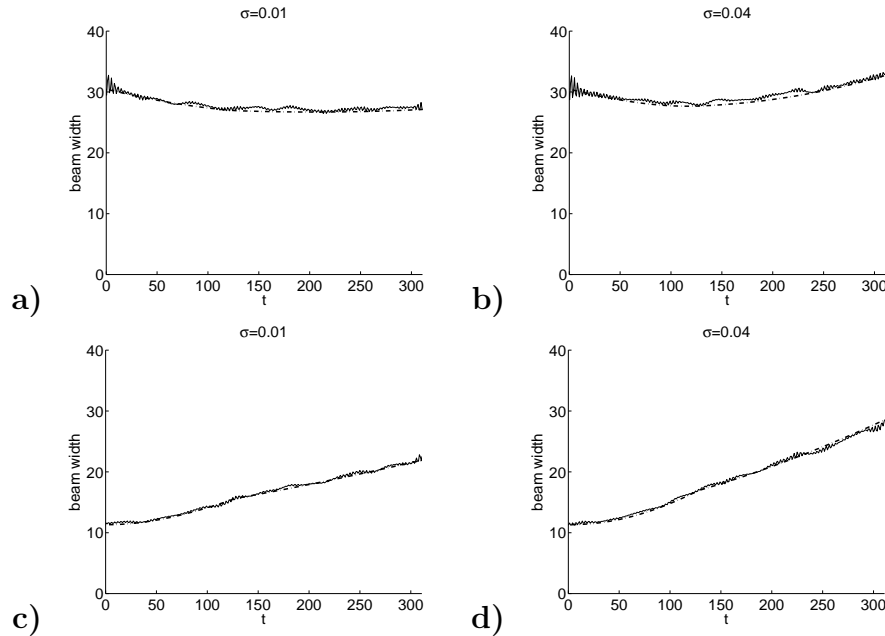


Figure 4. The rms reflected beam widths as a function of time for the unchirped incoming beam, $\sigma = 0.01$ (a), the chirped incoming beam, $\sigma = 0.01$ (b), the unchirped incoming beam, $\sigma = 0.04$ (c), the chirped incoming beam, $\sigma = 0.04$ (d). The thin solid lines are the numerical results and the thick dashed lines the theoretical formulas (39) and (51). In the case $\sigma = 0.01$ random forward scattering is rather weak. In the case $\sigma = 0.04$ random forward scattering is rather strong.

$z_i = 64$):

$$\begin{aligned} \text{for } \sigma = 0.01: & \quad \hat{c}_0 \simeq 0.98, \quad \hat{c}_1 \simeq 0.72, \quad \hat{t}_i \simeq 118, \quad \hat{z}_i = \hat{c}_0 \hat{t}_i / 2 \simeq 58, \\ \text{for } \sigma = 0.04: & \quad \hat{c}_0 \simeq 0.97, \quad \hat{c}_1 \simeq 0.66, \quad \hat{t}_i \simeq 128, \quad \hat{z}_i = \hat{c}_0 \hat{t}_i / 2 \simeq 62. \end{aligned}$$

6.2. Detection of change in microstructure

We next carry out a series of simulations with the same numerical model as in the previous subsection, however, we now examine the impact of two different types of background variations: a jump in the standard deviation of the random fluctuations of the medium and a jump in the transverse correlation radius of the random fluctuations of the medium.

In Figure 5, the background velocity $c_0 = 1$ and the transverse correlation length $l_x = 10$ are constant, but the standard deviation σ of the medium fluctuations goes from 0.04 in the region $[0, 64]$ to 0.028 in the region $[64, 128]$. The change in σ can be clearly seen in the jump of the reflected power. This jump is smooth because the separation of scales is not strong enough, and the pulse width is not much smaller than the total travel time. As pointed out before, the resolution obtained with the use of the incoming beam (52) with the pulse shape $\text{sinc}(Bt)$ is of the order of $2\pi c_0/B \sim 40$.

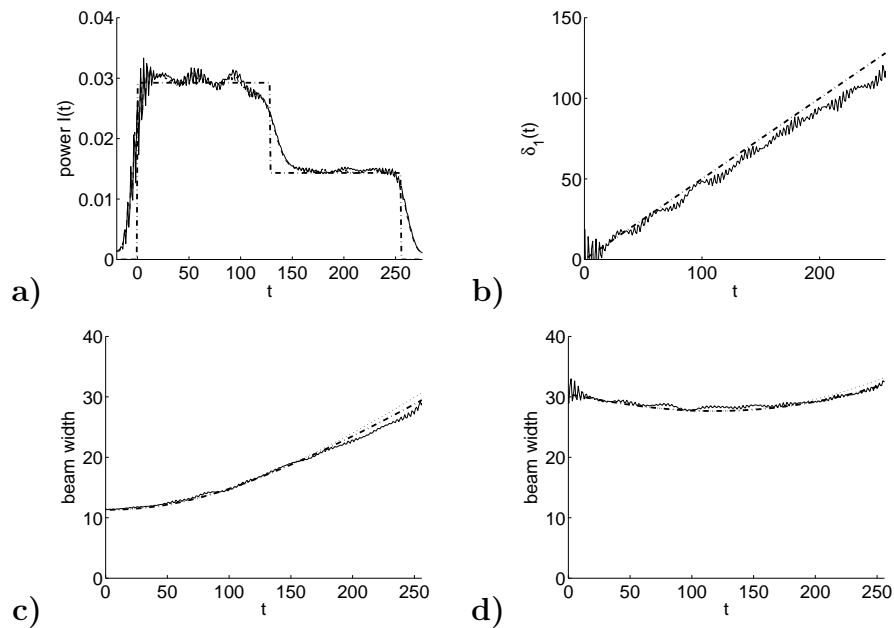


Figure 5. Characteristics of the reflected beam in the case of two heterogeneous layers with different standard deviations. Picture (a): the mean reflected power $I(t)$ for the unchirped and chirped incoming beams (the two thin lines are almost undistinguishable). The thick dashed is the theoretical formula (49). Picture (b): the difference $\delta_1(t)$. The thin solid lines are the numerical results and the thick dashed line stands the theoretical formula (53). Picture (c): the reflected beam radius for the unchirped beam. Picture (d): the reflected beam radius for the chirped beam. The thin solid lines are the numerical results and the thick dashed lines represents the theoretical formulas (39) and (51). The faint dotted lines are the theoretical radii if the standard deviation were 0.04 everywhere.

In Figure 6, the background velocity $c_0 = 1$ and the standard deviation $\sigma = 0.04$ are constant, but the transverse correlation of the medium fluctuations goes from $l_x = 8$ in the region $[0, 64]$ to $l_x = 16$ in the region $[64, 128]$. In this case the reflected power is constant and the change in l_x can be seen in the jump of the mean radius.

7. Conclusions

We have presented a theoretical framework that in particular can be used to characterize the spectrum of waves reflected by a random halfspace. We consider here the case when the reflected wave is weak and incoherent, corresponding to the absence of strong reflectors in the medium. We analyze how central quantities such as wave intensity, beam width and spectral radius depend on the medium parameters. We carry out a set of numerical simulations that shows how this information can be used for imaging of the medium. The simulations are carried out using a novel numerical scheme that is based on the analytic decomposition of the wave field used in this paper. The simulations demonstrate that indeed information about the medium can be inferred

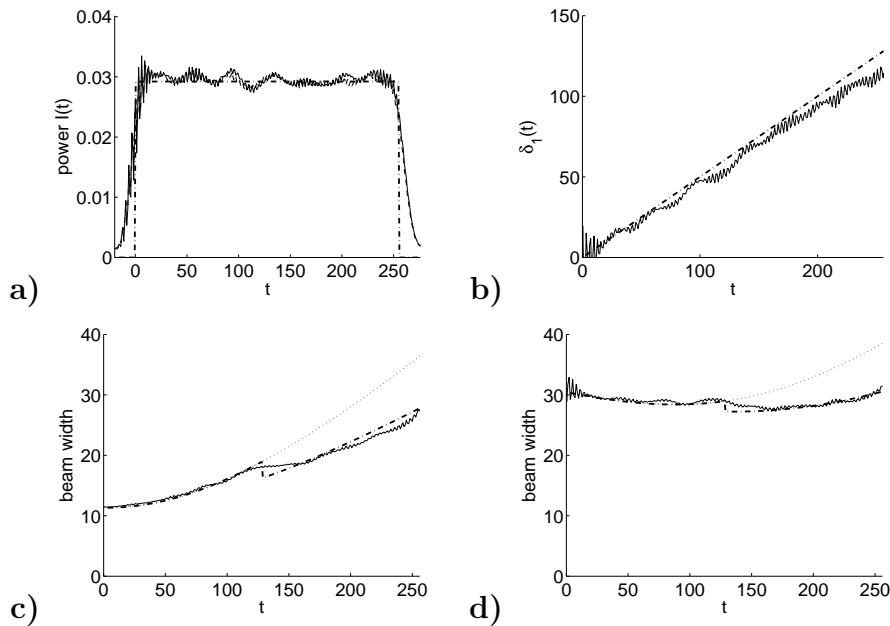


Figure 6. Characteristics of the reflected beam in the case of two heterogeneous layers with different transverse correlation radii. The subplots are defined as in Figure 5. The faint dotted lines in pictures (c) and (d) are the theoretical radii if the correlation radius were $l_x = 8$ everywhere.

from the spectrum of the reflections. In particular we are able to detect the depth at which the correlation radius of the medium fluctuations changes by looking at the time dynamics of the reflected wave. The analytic framework we have presented is important for dealing with such an inverse problem where the useful information is fully contained in the wave spectrum.

Acknowledgements

This work was supported by ONR grant N00014-02-1-0089 and DARPA grant N00014-05-1-0442. K. Sølna was supported by NSF grant DMS0307011 and the Sloan Foundation.

A. The generalized system of transport equations

In this appendix we write the system of transport equations that determines the moments of the reflection operator. The next proposition generalizes the result obtained in [8] to the case in which the medium is absorbing and has slow variations of the background velocity and impedance. It shows that it is possible to compute the cross moments of the reflection operator using diffusion approximation theory in the white noise limit $\varepsilon \rightarrow 0$.

Proposition A.1 *Let us introduce some notations: If $\boldsymbol{\kappa}_p(j), \boldsymbol{\kappa}'_p(j) \in \mathbb{R}^d$, $j = 1, \dots, n_{\mathbf{p}}$, then the multi-vector \mathbf{p} is the set*

$$\mathbf{p} = \{(\boldsymbol{\kappa}_p(j), \boldsymbol{\kappa}'_p(j))\}_{j=1}^{n_{\mathbf{p}}}, \quad (54)$$

where $n_{\mathbf{p}}$ stands for the number of pairs of \mathbf{p} . We introduce the high-order moments of products of $\widehat{\mathcal{R}}^\varepsilon(\omega, z, \boldsymbol{\kappa}, \boldsymbol{\kappa}')$, the reflection process, at two nearby frequencies:

$$\begin{aligned} \mathcal{U}_{\mathbf{p}, \mathbf{q}}^\varepsilon(\omega, h, z) = & \quad (55) \\ & \mathbb{E} \left[\prod_{j=1}^{n_{\mathbf{p}}} \widehat{\mathcal{R}}^\varepsilon \left(\omega + \frac{\varepsilon^2 h}{2}, z, \boldsymbol{\kappa}_p(j), \boldsymbol{\kappa}'_p(j) \right) \prod_{l=1}^{n_{\mathbf{q}}} \overline{\widehat{\mathcal{R}}^\varepsilon} \left(\omega - \frac{\varepsilon^2 h}{2}, z, \boldsymbol{\kappa}_q(l), \boldsymbol{\kappa}'_q(l) \right) \right], \end{aligned}$$

where \mathbf{p}, \mathbf{q} are two multi-vectors of the form (54). We define the autocorrelation function of the fluctuations of the medium by (2) and its Fourier transform by (24) and

$$\widehat{C}^\pm(z, k, \boldsymbol{\kappa}) = 2 \int_{\mathbb{R}^d} \int_0^\infty C(z, z', \mathbf{x}') e^{\pm i k z' - i \boldsymbol{\kappa} \cdot \mathbf{x}'} dz' d\mathbf{x}'. \quad (56)$$

The family of Fourier transforms

$$W_{\mathbf{p}, \mathbf{q}}^\varepsilon(\omega, \tau, z) = \frac{1}{2\pi} \int e^{-i h [\tau - (n_{\mathbf{p}} + n_{\mathbf{q}}) \tau_0(z)]} \mathcal{U}_{\mathbf{p}, \mathbf{q}}^\varepsilon(\omega, h, z) dh, \quad (57)$$

converges as $\varepsilon \rightarrow 0$ to the solution $W_{\mathbf{p}, \mathbf{q}}$ of the system of transport equations

$$\begin{aligned} \frac{\partial W_{\mathbf{p}, \mathbf{q}}}{\partial z} + \frac{n_{\mathbf{p}} + n_{\mathbf{q}}}{c_0(z)} \frac{\partial W_{\mathbf{p}, \mathbf{q}}}{\partial \tau} = & - \frac{\gamma_0(z)}{\zeta_0(z)} (n_{\mathbf{p}} + n_{\mathbf{q}}) W_{\mathbf{p}, \mathbf{q}} + \frac{i c_0(z)}{2\omega} \Phi_{\mathbf{p}, \mathbf{q}} W_{\mathbf{p}, \mathbf{q}} \\ & + \frac{\omega^2}{4(2\pi)^d c_0^2(z)} (\mathcal{L}_W W)_{\mathbf{p}, \mathbf{q}}, \end{aligned} \quad (58)$$

with the initial conditions $W_{\mathbf{p}, \mathbf{q}}(\omega, \tau, z = 0) = \mathbf{1}_0(n_{\mathbf{p}}) \mathbf{1}_0(n_{\mathbf{q}}) \delta(\tau)$. Here we have defined

$$\Phi_{\mathbf{p}, \mathbf{q}} = - \sum_{j=1}^{n_{\mathbf{p}}} (|\boldsymbol{\kappa}_p(j)|^2 + |\boldsymbol{\kappa}'_p(j)|^2) + \sum_{l=1}^{n_{\mathbf{q}}} (|\boldsymbol{\kappa}_q(l)|^2 + |\boldsymbol{\kappa}'_q(l)|^2), \quad (59)$$

and the operator \mathcal{L}_W is given by

$$\begin{aligned} (\mathcal{L}_W W)_{\mathbf{p}, \mathbf{q}} = & - \int \left[n_{\mathbf{p}} \widehat{C}^+(z, 2k, \boldsymbol{\kappa}) + n_{\mathbf{q}} \widehat{C}^-(z, 2k, \boldsymbol{\kappa}) + (n_{\mathbf{p}} + n_{\mathbf{q}}) \widehat{C}(z, 0, \boldsymbol{\kappa}) \right] d\boldsymbol{\kappa} W_{\mathbf{p}, \mathbf{q}} \\ & - \int \widehat{C}(z, 0, \boldsymbol{\kappa}) \left[\sum_{j=1}^{n_{\mathbf{p}}} W_{\mathbf{p}, \mathbf{q}} \{ |j|(\boldsymbol{\kappa}_p(j) - \boldsymbol{\kappa}, \boldsymbol{\kappa}'_p(j) - \boldsymbol{\kappa}) \}, \mathbf{q} + \sum_{l=1}^{n_{\mathbf{q}}} W_{\mathbf{p}, \mathbf{q}} \{ |l|(\boldsymbol{\kappa}_q(l) - \boldsymbol{\kappa}, \boldsymbol{\kappa}'_q(l) - \boldsymbol{\kappa}) \} \right] d\boldsymbol{\kappa} \\ & - \sum_{j_1 \neq j_2 = 1}^{n_{\mathbf{p}}} \int \left\{ \widehat{C}(z, 2k, \boldsymbol{\kappa}_p(j_1) - \boldsymbol{\kappa}'_p(j_1)) W_{\mathbf{p}, \mathbf{q}} \{ |j_1, j_2|(\boldsymbol{\kappa}_p(j_2), \boldsymbol{\kappa} - \boldsymbol{\kappa}_p(j_1)), (\boldsymbol{\kappa} - \boldsymbol{\kappa}'_p(j_1), \boldsymbol{\kappa}'_p(j_2)) \}, \mathbf{q} \right. \\ & + \frac{1}{2} \widehat{C}(z, 0, \boldsymbol{\kappa}) \left[W_{\mathbf{p}, \mathbf{q}} \{ |j_1, j_2|(\boldsymbol{\kappa}_p(j_1) - \boldsymbol{\kappa}, \boldsymbol{\kappa}'_p(j_1)), (\boldsymbol{\kappa}_p(j_2) + \boldsymbol{\kappa}, \boldsymbol{\kappa}'_p(j_2)) \}, \mathbf{q} \right. \\ & + 2W_{\mathbf{p}, \mathbf{q}} \{ |j_1, j_2|(\boldsymbol{\kappa}_p(j_1) - \boldsymbol{\kappa}, \boldsymbol{\kappa}'_p(j_1)), (\boldsymbol{\kappa}_p(j_2), \boldsymbol{\kappa}'_p(j_2) - \boldsymbol{\kappa}) \}, \mathbf{q} \\ & \left. \left. + W_{\mathbf{p}, \mathbf{q}} \{ |j_1, j_2|(\boldsymbol{\kappa}_p(j_1), \boldsymbol{\kappa}'_p(j_1) - \boldsymbol{\kappa}), (\boldsymbol{\kappa}_p(j_2), \boldsymbol{\kappa}'_p(j_2) + \boldsymbol{\kappa}) \}, \mathbf{q} \right] \right\} d\boldsymbol{\kappa} \\ & - \sum_{l_1 \neq l_2 = 1}^{n_{\mathbf{q}}} \int \left\{ \widehat{C}(z, 2k, \boldsymbol{\kappa}_q(l_1) - \boldsymbol{\kappa}'_q(l_1)) W_{\mathbf{p}, \mathbf{q}} \{ |l_1, l_2|(\boldsymbol{\kappa}_q(l_2), \boldsymbol{\kappa} - \boldsymbol{\kappa}_q(l_1)), (\boldsymbol{\kappa} - \boldsymbol{\kappa}'_q(l_1), \boldsymbol{\kappa}'_q(l_2)) \} \right. \end{aligned}$$

$$\begin{aligned}
& + \frac{1}{2} \widehat{C}(z, 0, \boldsymbol{\kappa}) \left[W_{\mathbf{p}, \mathbf{q}} \{ |l_1, l_2| (\boldsymbol{\kappa}_q(l_1) - \boldsymbol{\kappa}, \boldsymbol{\kappa}'_q(l_1)), (\boldsymbol{\kappa}_q(l_2) + \boldsymbol{\kappa}, \boldsymbol{\kappa}'_q(l_2)) \} \right. \\
& + 2W_{\mathbf{p}, \mathbf{q}} \{ |l_1, l_2| (\boldsymbol{\kappa}_q(l_1) - \boldsymbol{\kappa}, \boldsymbol{\kappa}'_q(l_1)), (\boldsymbol{\kappa}_q(l_2), \boldsymbol{\kappa}'_q(l_2) - \boldsymbol{\kappa}) \} \\
& \left. + W_{\mathbf{p}, \mathbf{q}} \{ |l_1, l_2| (\boldsymbol{\kappa}_q(l_1), \boldsymbol{\kappa}'_q(l_1) - \boldsymbol{\kappa}), (\boldsymbol{\kappa}_q(l_2), \boldsymbol{\kappa}'_q(l_2) + \boldsymbol{\kappa}) \} \right] d\boldsymbol{\kappa} \\
& + \sum_{j=1}^{n_{\mathbf{p}}} \sum_{l=1}^{n_{\mathbf{q}}} \left\{ \widehat{C}(z, 2k, \boldsymbol{\kappa}_p(j) - \boldsymbol{\kappa}'_p(j)) \delta(\boldsymbol{\kappa}_p(j) - \boldsymbol{\kappa}'_p(j) - \boldsymbol{\kappa}_q(l) + \boldsymbol{\kappa}'_q(l)) W_{\mathbf{p}|j, \mathbf{q}|l} + \int \widehat{C}(z, 0, \boldsymbol{\kappa}) \right. \\
& \times \left[W_{\mathbf{p}} \{ |j| (\boldsymbol{\kappa}_p(j) - \boldsymbol{\kappa}, \boldsymbol{\kappa}'_p(j)) \}, \mathbf{q} \{ |l| (\boldsymbol{\kappa}_q(l) - \boldsymbol{\kappa}, \boldsymbol{\kappa}'_q(l)) \} + W_{\mathbf{p}} \{ |j| (\boldsymbol{\kappa}_p(j), \boldsymbol{\kappa}'_p(j) - \boldsymbol{\kappa}) \}, \mathbf{q} \{ |l| (\boldsymbol{\kappa}_q(l), \boldsymbol{\kappa}'_q(l) - \boldsymbol{\kappa}) \} \right. \\
& \left. + W_{\mathbf{p}} \{ |j| (\boldsymbol{\kappa}_p(j) - \boldsymbol{\kappa}, \boldsymbol{\kappa}'_p(j)) \}, \mathbf{q} \{ |l| (\boldsymbol{\kappa}_q(l), \boldsymbol{\kappa}'_q(l) + \boldsymbol{\kappa}) \} + W_{\mathbf{p}} \{ |j| (\boldsymbol{\kappa}_p(j), \boldsymbol{\kappa}'_p(j) - \boldsymbol{\kappa}) \}, \mathbf{q} \{ |l| (\boldsymbol{\kappa}_q(l) + \boldsymbol{\kappa}, \boldsymbol{\kappa}'_q(l)) \} \right] d\boldsymbol{\kappa} \\
& \left. + \int \int \int \widehat{C}(z, 2k, \boldsymbol{\kappa}_1) W_{\mathbf{p}} \{ |j| (\boldsymbol{\kappa}_p(j), \boldsymbol{\kappa}_2), (\boldsymbol{\kappa}_2 - \boldsymbol{\kappa}_1, \boldsymbol{\kappa}'_p(j)) \}, \mathbf{q} \{ |l| (\boldsymbol{\kappa}_q(l), \boldsymbol{\kappa}_3), (\boldsymbol{\kappa}_3 - \boldsymbol{\kappa}_1, \boldsymbol{\kappa}'_q(l)) \} d\boldsymbol{\kappa}_1 d\boldsymbol{\kappa}_2 d\boldsymbol{\kappa}_3 \right\},
\end{aligned}$$

where $k = \omega/c_0(z)$ and we have used the notations:

$$\mathbf{p}|j = \{ (\boldsymbol{\kappa}_p(j'), \boldsymbol{\kappa}'_p(j')) \}_{j'=1 \neq j}^{n_{\mathbf{p}}}, \quad \mathbf{p}\{|j|(\boldsymbol{\kappa}_1, \boldsymbol{\kappa}_2)\} = \{ (\boldsymbol{\kappa}_p(j'), \boldsymbol{\kappa}'_p(j')) \}_{j'=1 \neq j}^{n_{\mathbf{p}}} \cup (\boldsymbol{\kappa}_1, \boldsymbol{\kappa}_2).$$

The proof of the proposition follows exactly the one of Ref. [8] in which the medium was not absorbing and had no slow variation of the background velocity and impedance.

In the weak backscattering regime (23) we have

$$W_{\mathbf{p}, \mathbf{q}} = \begin{cases} \mathcal{O}(1) & \text{if } n_{\mathbf{p}} = n_{\mathbf{q}} = 0, \\ \mathcal{O}(\delta) & \text{if } n_{\mathbf{p}} = n_{\mathbf{q}} = 1, \\ \mathcal{O}(\delta^2) & \text{otherwise.} \end{cases}$$

We have up to terms of order δ^2 :

$$\begin{aligned}
& \frac{\partial W_{(\boldsymbol{\kappa}_1, \boldsymbol{\kappa}_2), (\boldsymbol{\kappa}_3, \boldsymbol{\kappa}_4)}}{\partial z} + \frac{2}{c_0(z)} \frac{\partial W_{(\boldsymbol{\kappa}_1, \boldsymbol{\kappa}_2), (\boldsymbol{\kappa}_3, \boldsymbol{\kappa}_4)}}{\partial \tau} = -\frac{2\gamma_0(z)}{\zeta_0(z)} W_{(\boldsymbol{\kappa}_1, \boldsymbol{\kappa}_2), (\boldsymbol{\kappa}_3, \boldsymbol{\kappa}_4)} \\
& + \frac{ic_0(z)}{2\omega} \left[(|\boldsymbol{\kappa}_3|^2 + |\boldsymbol{\kappa}_4|^2) - (|\boldsymbol{\kappa}_1|^2 + |\boldsymbol{\kappa}_2|^2) \right] W_{(\boldsymbol{\kappa}_1, \boldsymbol{\kappa}_2), (\boldsymbol{\kappa}_3, \boldsymbol{\kappa}_4)} \\
& + \frac{\omega^2}{4(2\pi)^d c_0^2(z)} \int \widehat{C}(z, 0, \boldsymbol{\kappa}) \left\{ W_{(\boldsymbol{\kappa}_1 - \boldsymbol{\kappa}, \boldsymbol{\kappa}_2), (\boldsymbol{\kappa}_3 - \boldsymbol{\kappa}, \boldsymbol{\kappa}_4)} + W_{(\boldsymbol{\kappa}_1, \boldsymbol{\kappa}_2 - \boldsymbol{\kappa}), (\boldsymbol{\kappa}_3, \boldsymbol{\kappa}_4 - \boldsymbol{\kappa})} \right. \\
& \quad + W_{(\boldsymbol{\kappa}_1 - \boldsymbol{\kappa}, \boldsymbol{\kappa}_2), (\boldsymbol{\kappa}_3, \boldsymbol{\kappa}_4 + \boldsymbol{\kappa})} + W_{(\boldsymbol{\kappa}_1, \boldsymbol{\kappa}_2 - \boldsymbol{\kappa}), (\boldsymbol{\kappa}_3 + \boldsymbol{\kappa}, \boldsymbol{\kappa}_4)} \\
& \quad \left. - W_{(\boldsymbol{\kappa}_1 - \boldsymbol{\kappa}, \boldsymbol{\kappa}_2 - \boldsymbol{\kappa}), (\boldsymbol{\kappa}_3, \boldsymbol{\kappa}_4)} - W_{(\boldsymbol{\kappa}_1, \boldsymbol{\kappa}_2), (\boldsymbol{\kappa}_3 - \boldsymbol{\kappa}, \boldsymbol{\kappa}_4 - \boldsymbol{\kappa})} - 2W_{(\boldsymbol{\kappa}_1, \boldsymbol{\kappa}_2), (\boldsymbol{\kappa}_3, \boldsymbol{\kappa}_4)} \right\} d\boldsymbol{\kappa} \\
& + \frac{\omega^2}{4(2\pi)^d c_0^2(z)} \widehat{C}\left(z, \frac{2\omega}{c_0(z)}, \boldsymbol{\kappa}_1 - \boldsymbol{\kappa}_2\right) \delta(\boldsymbol{\kappa}_1 - \boldsymbol{\kappa}_2 - \boldsymbol{\kappa}_3 + \boldsymbol{\kappa}_4) \delta(\tau), \tag{60}
\end{aligned}$$

with $W_{(\boldsymbol{\kappa}_1, \boldsymbol{\kappa}_2), (\boldsymbol{\kappa}_3, \boldsymbol{\kappa}_4)}(\omega, \tau, z = 0) = 0$. Note that the coupling terms preserve the sum $\boldsymbol{\kappa}_1 - \boldsymbol{\kappa}_2 - \boldsymbol{\kappa}_3 + \boldsymbol{\kappa}_4$. Therefore $W_{(\boldsymbol{\kappa}_1, \boldsymbol{\kappa}_2), (\boldsymbol{\kappa}_3, \boldsymbol{\kappa}_4)}$ is supported on $\boldsymbol{\kappa}_1 - \boldsymbol{\kappa}_2 - \boldsymbol{\kappa}_3 + \boldsymbol{\kappa}_4 = \mathbf{0}$ and we can write the solution in terms of three ‘‘effective’’ wavevectors. By parameterizing the remaining three wavevectors in a suitable form we obtain the statement of Proposition 3.1.

B. The system for the dimensionless density

In this appendix we introduce a dimensionless formulation of the system of equations that determines the cross spectral density V defined in Proposition 3.1. The

autocorrelation function C of the fluctuations of the medium is defined by (2). We introduce the dimensionless autocorrelation function \mathcal{C} of the random medium:

$$C(z, z', \mathbf{x}') = \sigma^2 \mathcal{C}\left(\frac{z}{L}, \frac{z'}{l_z}, \frac{\mathbf{x}'}{l_x}\right),$$

where l_z (respectively l_x) is the longitudinal (respectively transverse) correlation radius of the random fluctuations, and σ is the standard deviation of the fluctuations. We denote by $\widehat{\mathcal{C}}(\tilde{z}, K, \boldsymbol{\mu})$ and by $\check{\mathcal{C}}(\tilde{z}, K, \boldsymbol{\lambda})$ the full and partial Fourier transforms

$$\widehat{\mathcal{C}}(\tilde{z}, K, \boldsymbol{\mu}) = \int \int_{-\infty}^{\infty} \mathcal{C}(\tilde{z}, \tilde{z}', \boldsymbol{\lambda}) e^{-iK\tilde{z}' - i\boldsymbol{\mu} \cdot \boldsymbol{\lambda}} d\tilde{z}' d\boldsymbol{\lambda}, \quad (61)$$

$$\check{\mathcal{C}}(\tilde{z}, K, \boldsymbol{\lambda}) = \int_{-\infty}^{\infty} \mathcal{C}(\tilde{z}, \tilde{z}', \boldsymbol{\lambda}) e^{-iK\tilde{z}'} d\tilde{z}'. \quad (62)$$

We introduce the dimensionless profiles $\tilde{c}_0(\tilde{z})$, $\tilde{\zeta}_0(\tilde{z})$, and $\tilde{\gamma}_0(\tilde{z})$:

$$c_0(z) = \bar{c} \tilde{c}_0\left(\frac{z}{L}\right), \quad \zeta_0(z) = \bar{\zeta} \tilde{\zeta}_0\left(\frac{z}{L}\right), \quad \gamma_0(z) = \bar{\gamma} \tilde{\gamma}_0\left(\frac{z}{L}\right), \quad (63)$$

where \bar{c} , $\bar{\zeta}$, and $\bar{\gamma}$ are typical speed of sound, impedance and absorption coefficients. We also define the dimensionless functions

$$\tilde{J}_0(\tilde{z}) = \int_0^{\tilde{z}} \tilde{c}_0(\tilde{z}') d\tilde{z}', \quad \tilde{G}_0(\tilde{z}) = \int_0^{\tilde{z}} \frac{\tilde{\gamma}_0(\tilde{z}')}{\tilde{\zeta}_0(\tilde{z}')} d\tilde{z}', \quad \tilde{\tau}_0(\tilde{z}) = \int_0^{\tilde{z}} \frac{1}{\tilde{c}_0(\tilde{z}')} d\tilde{z}'. \quad (64)$$

We consider the Fourier transform D of the cross spectral density V

$$V_{\boldsymbol{\kappa}_u, \boldsymbol{\kappa}_v, \boldsymbol{\kappa}_w}(\omega, \tau, z) = \frac{1}{2\pi} \int D(\omega, h, z, \boldsymbol{\kappa}_u, \boldsymbol{\kappa}_v, \boldsymbol{\kappa}_w) e^{-ih\tau} dh. \quad (65)$$

The following proposition shows that the parameters α and β defined by (33) determine the evolution of D .

Proposition B.1 *The density D is given by*

$$D(\omega, h, z, \boldsymbol{\kappa}_u, \boldsymbol{\kappa}_v, \boldsymbol{\kappa}_w) = \bar{D} \mathcal{D}\left(\frac{\omega}{\omega_0}, \frac{hL}{\bar{c}}, \frac{z}{L}, \boldsymbol{\kappa}_u l_x, \boldsymbol{\kappa}_v l_x, \boldsymbol{\kappa}_w l_x\right) \\ \times \exp\left[2i \frac{hL}{\bar{c}} \tilde{\tau}_0\left(\frac{z}{L}\right) - \bar{G} \tilde{G}_0\left(\frac{z}{L}\right) - i \boldsymbol{\kappa}_u \cdot \boldsymbol{\kappa}_v \frac{\bar{c}L}{\omega} \tilde{J}_0\left(\frac{z}{L}\right)\right], \quad (66)$$

with

$$\bar{D} = \frac{\omega_0^2 \sigma^2 l_z l_x^d L}{4(2\pi)^d \bar{c}^2}, \quad \bar{G} = \frac{2\bar{\sigma}L}{\bar{\zeta}}.$$

The frequencies $\tilde{\omega}$ and \tilde{h} are frozen parameters in the equation satisfied by the dimensionless density $\mathcal{D}(\tilde{\omega}, \tilde{h}, \tilde{z}, \mathbf{u}, \mathbf{v}, \mathbf{w})$:

$$\frac{d\mathcal{D}(\tilde{\omega}, \tilde{h}, \tilde{z}, \mathbf{u}, \mathbf{v}, \mathbf{w})}{d\tilde{z}} = \tilde{\omega}^2 \widehat{\mathcal{B}}_{2\tilde{\omega}}(\tilde{z}, \mathbf{w}) e^{i\frac{\alpha}{\tilde{\omega}} \mathbf{u} \cdot \mathbf{v} \tilde{J}_0(\tilde{z})} e^{-2i\tilde{h}\tilde{\tau}_0(\tilde{z})} e^{\bar{G}\tilde{G}_0(\tilde{z})} + \frac{\beta \tilde{\omega}^2}{(2\pi)^d} \int \widehat{\mathcal{B}}_0(\tilde{z}, \boldsymbol{\mu}) \\ \times \left[e^{i\frac{\alpha}{\tilde{\omega}} \boldsymbol{\mu} \cdot \mathbf{v} \tilde{J}_0(\tilde{z})} \mathcal{D}(\tilde{\omega}, \tilde{h}, \tilde{z}, \mathbf{u} - \boldsymbol{\mu}, \mathbf{v}, \mathbf{w} + \boldsymbol{\mu}) + e^{-i\frac{\alpha}{\tilde{\omega}} \boldsymbol{\mu} \cdot \mathbf{v} \tilde{J}_0(\tilde{z})} \mathcal{D}(\tilde{\omega}, \tilde{h}, \tilde{z}, \mathbf{u} + \boldsymbol{\mu}, \mathbf{v}, \mathbf{w} + \boldsymbol{\mu}) \right. \\ \left. + e^{i\frac{\alpha}{\tilde{\omega}} \boldsymbol{\mu} \cdot \mathbf{u} \tilde{J}_0(\tilde{z})} \mathcal{D}(\tilde{\omega}, \tilde{h}, \tilde{z}, \mathbf{u}, \mathbf{v} - \boldsymbol{\mu}, \mathbf{w} + \boldsymbol{\mu}) + e^{-i\frac{\alpha}{\tilde{\omega}} \boldsymbol{\mu} \cdot \mathbf{u} \tilde{J}_0(\tilde{z})} \mathcal{D}(\tilde{\omega}, \tilde{h}, \tilde{z}, \mathbf{u}, \mathbf{v} + \boldsymbol{\mu}, \mathbf{w} + \boldsymbol{\mu}) \right. \\ \left. - e^{-i\frac{\alpha}{\tilde{\omega}} [\boldsymbol{\mu} \cdot \mathbf{u} + \boldsymbol{\mu} \cdot (\mathbf{v} + \boldsymbol{\mu})] \tilde{J}_0(\tilde{z})} \mathcal{D}(\tilde{\omega}, \tilde{h}, \tilde{z}, \mathbf{u} + \boldsymbol{\mu}, \mathbf{v} + \boldsymbol{\mu}, \mathbf{w}) \right. \\ \left. - e^{-i\frac{\alpha}{\tilde{\omega}} [\boldsymbol{\mu} \cdot \mathbf{u} - \boldsymbol{\mu} \cdot (\mathbf{v} + \boldsymbol{\mu})] \tilde{J}_0(\tilde{z})} \mathcal{D}(\tilde{\omega}, \tilde{h}, \tilde{z}, \mathbf{u} - \boldsymbol{\mu}, \mathbf{v} + \boldsymbol{\mu}, \mathbf{w}) - 2\mathcal{D}(\tilde{\omega}, \tilde{h}, \tilde{z}, \mathbf{u}, \mathbf{v}, \mathbf{w}) \right] d\boldsymbol{\mu}, \quad (67)$$

starting from $\mathcal{D}(\tilde{z} = 0, \mathbf{u}, \mathbf{v}, \mathbf{w}) = 0$, where

$$\hat{\mathcal{B}}_{\tilde{\omega}}(\tilde{z}, \mathbf{w}) = \frac{1}{\tilde{c}_0^2(\tilde{z})} \hat{\mathcal{C}}\left(\tilde{z}, \frac{\omega_0 l_z}{\tilde{c}_0(\tilde{z})} \tilde{\omega}, \mathbf{w}\right). \quad (68)$$

C. Proof of Proposition 3.2

The mean reflected intensity $I^\varepsilon(t)$ has the limit $I(t)$ as $\varepsilon \rightarrow 0$:

$$I(t) = \frac{1}{(2\pi)^{d+1}} \int \cdots \int W_{(\boldsymbol{\kappa}_1, \boldsymbol{\kappa}_2), (\boldsymbol{\kappa}_1, \boldsymbol{\kappa}_4)}(\omega, t, L) \hat{b}_{\text{inc}}(\omega, \boldsymbol{\kappa}_2) \overline{\hat{b}_{\text{inc}}(\omega, \boldsymbol{\kappa}_4)} d\boldsymbol{\kappa}_1 d\boldsymbol{\kappa}_2 d\boldsymbol{\kappa}_4 d\omega.$$

Using the identity (66), this can be expressed as

$$\begin{aligned} I(t) &= \frac{1}{(2\pi)^{d+1}} \int \cdots \int D(\omega, h, L, \mathbf{0}, \boldsymbol{\kappa} + 2\boldsymbol{\kappa}', \boldsymbol{\kappa}) d\boldsymbol{\kappa} e^{-iht} |\hat{b}_{\text{inc}}(\omega, \boldsymbol{\kappa}')|^2 d\boldsymbol{\kappa}' dh d\omega \\ &= \frac{\bar{D}}{(2\pi)^{d+2}} \int \int \int \mathcal{E}\left(\frac{\omega}{\omega_0}, \frac{hL}{\bar{c}}, 1, 2\boldsymbol{\kappa}' l_x\right) e^{2i\frac{hL}{\bar{c}}\tilde{\tau}_0(1) - iht} e^{-\bar{G}\bar{G}_0(1)} |\hat{b}_{\text{inc}}(\omega, \boldsymbol{\kappa}')|^2 d\boldsymbol{\kappa}' dh d\omega, \end{aligned} \quad (69)$$

where

$$\mathcal{E}(\tilde{\omega}, \tilde{h}, \tilde{z}, \mathbf{v}) = \int \mathcal{D}(\tilde{\omega}, \tilde{h}, \tilde{z}, \mathbf{0}, \mathbf{w} + 2\mathbf{v}, \mathbf{w}) d\mathbf{w}.$$

Then, using the system of coupled differential equations (67), we get that the quantity $\mathcal{E}(\tilde{\omega}, \tilde{h}, \tilde{z}, \mathbf{v})$ satisfies

$$\begin{aligned} \frac{d\mathcal{E}(\tilde{\omega}, \tilde{h}, \tilde{z}, \mathbf{v})}{d\tilde{z}} &= (2\pi)^d \tilde{\omega}^2 \check{\mathcal{B}}_{2\tilde{\omega}}(\tilde{z}, \mathbf{0}) e^{\bar{G}\bar{G}_0(\tilde{z})} e^{-2i\tilde{h}\tilde{\tau}_0(\tilde{z})} \\ &\quad + \frac{\beta \tilde{\omega}^2}{(2\pi)^d} \int \hat{\mathcal{B}}_0(\tilde{z}, \boldsymbol{\mu}) \left[\mathcal{E}(\tilde{\omega}, \tilde{h}, \tilde{z}, \mathbf{v} + \boldsymbol{\mu}) - \mathcal{E}(\tilde{\omega}, \tilde{h}, \tilde{z}, \mathbf{v}) \right] d\boldsymbol{\mu}, \end{aligned}$$

because all but two terms proportional to β in the right-hand side of (66) cancel each other when taking $(\mathbf{u}, \mathbf{v}, \mathbf{w}) \rightarrow (\mathbf{0}, \mathbf{w} + 2\mathbf{v}, \mathbf{w})$ and integrating in \mathbf{w} . Here $\check{\mathcal{B}}_{\tilde{\omega}}(\tilde{z}, \boldsymbol{\lambda})$ is the inverse Fourier transform of $\hat{\mathcal{B}}_{\tilde{\omega}}(\tilde{z}, \mathbf{w})$:

$$\check{\mathcal{B}}_{\tilde{\omega}}(\tilde{z}, \boldsymbol{\lambda}) = \frac{1}{\tilde{c}_0^2(\tilde{z})} \check{\mathcal{C}}\left(\tilde{z}, \frac{\omega_0 l_z}{\tilde{c}_0(\tilde{z})} \tilde{\omega}, \boldsymbol{\lambda}\right). \quad (70)$$

The initial condition for the differential equation for \mathcal{E} is $\mathcal{E}(\tilde{\omega}, \tilde{h}, \tilde{z} = 0, \mathbf{v}) = 0$. The solution is the function

$$\mathcal{E}(\tilde{\omega}, \tilde{h}, \tilde{z}, \mathbf{v}) = (2\pi)^d \tilde{\omega}^2 \int_0^{\tilde{z}} \check{\mathcal{B}}_{2\tilde{\omega}}(\tilde{z}', \mathbf{0}) e^{\bar{G}\bar{G}_0(\tilde{z}')} e^{-2i\tilde{h}\tilde{\tau}_0(\tilde{z}')} d\tilde{z}',$$

which is independent of \mathbf{v} . We next substitute in (69) and integrate with respect to h . The integral in h generates a delta distribution:

$$\begin{aligned} I(t) &= \frac{\bar{D}}{2\pi l_x^d} \int \int_0^1 \delta\left(t - \frac{2L}{\bar{c}}(\tilde{\tau}_0(1) - \tilde{\tau}_0(\tilde{z}))\right) \frac{\omega^2}{\omega_0^2} \check{\mathcal{B}}_{2\frac{\omega}{\omega_0}}(\tilde{z}, \mathbf{0}) \\ &\quad \times e^{\bar{G}(\bar{G}_0(\tilde{z}) - \bar{G}_0(1))} \left[\int |\hat{b}_{\text{inc}}(\omega, \boldsymbol{\kappa}')|^2 d\boldsymbol{\kappa}' \right] d\tilde{z} d\omega. \end{aligned}$$

The delta distribution concentrates the integrand on a particular value of \tilde{z} :

$$I(t) = \frac{\bar{D}\bar{c}}{4\pi l_x^d L} \int \tilde{c}_0(\tilde{z}(t)) \frac{\omega^2}{\omega_0^2} \tilde{\mathcal{B}}_{2\frac{\omega}{\omega_0}}(\tilde{z}(t), \mathbf{0}) e^{\bar{G}(\bar{G}_0(\tilde{z}(t)) - \bar{G}_0(1))} \left[\int |\hat{b}_{\text{inc}}(\omega, \boldsymbol{\kappa}')|^2 d\boldsymbol{\kappa}' \right] d\omega,$$

where $\tilde{z}(t) \in (0, 1)$ is such that

$$\int_{\tilde{z}(t)}^L \frac{1}{\tilde{c}_0(\tilde{z}')} d\tilde{z}' = \frac{\bar{c}t}{2L}. \quad (71)$$

For comparison, the total input energy is (32). The expression of the intensity in the original variables is given by (28).

D. Asymptotic expressions for the cross spectral density

In the next two lemmas we give the asymptotic expressions for the dimensionless density \mathcal{D} in the regime $\alpha \gg 1$. They generalize the results obtained in [8]

Lemma D.1 (i) If $\mathbf{u} \cdot \mathbf{v} \neq 0$, then $\lim_{\alpha \rightarrow \infty} \mathcal{D}(\tilde{z}, \mathbf{u}, \mathbf{v}, \mathbf{w}) = 0$.

(ii) If $\mathbf{u} \neq \mathbf{0}$, $\mathbf{v} \neq \mathbf{0}$, and $\mathbf{u} \cdot \mathbf{v} = 0$, then

$$\lim_{\alpha \rightarrow \infty} \mathcal{D}(\tilde{z}, \tilde{\omega}, \tilde{h}, \mathbf{u}, \mathbf{v}, \mathbf{w}) = \int_0^{\tilde{z}} \tilde{\omega}^2 \hat{\mathcal{B}}_{2\tilde{\omega}}(\tilde{z}', \mathbf{w}) e^{-2i\tilde{h}\tilde{\tau}_0(\tilde{z}')} e^{\bar{G}\bar{G}_0(\tilde{z}')} e^{-2\beta\tilde{\omega}^2 \int_{\tilde{z}'}^{\tilde{z}} \tilde{\mathcal{B}}_0(\tilde{z}'', \mathbf{0}) d\tilde{z}''} d\tilde{z}'. \quad (72)$$

(iii) If $\mathbf{u} = \mathbf{0}$ and $\mathbf{v} \neq \mathbf{0}$, then $\lim_{\alpha \rightarrow \infty} \mathcal{D}(\tilde{z}, \tilde{\omega}, \tilde{h}, \mathbf{0}, \mathbf{v}, \mathbf{w}) = \mathcal{D}_0(\tilde{z}, \tilde{\omega}, \tilde{h}, \mathbf{w})$ where $\mathcal{D}_0(\tilde{z}, \tilde{\omega}, \tilde{h}, \mathbf{w})$ is the solution of

$$\frac{d\mathcal{D}_0}{d\tilde{z}} = \tilde{\omega}^2 \hat{\mathcal{B}}_{2\tilde{\omega}}(\tilde{z}, \mathbf{w}) e^{-2i\tilde{h}\tilde{\tau}_0(\tilde{z})} e^{\bar{G}\bar{G}_0(\tilde{z})} + \frac{2\beta\tilde{\omega}^2}{(2\pi)^d} \int \hat{\mathcal{B}}_0(\tilde{z}, \boldsymbol{\mu}) [\mathcal{D}_0(\mathbf{w} + \boldsymbol{\mu}) - \mathcal{D}_0(\mathbf{w})] d\boldsymbol{\mu}, \quad (73)$$

starting from $\mathcal{D}_0(\tilde{z} = 0, \tilde{\omega}, \tilde{h}, \mathbf{w}) = 0$.

(iv) If $\mathbf{u} \neq \mathbf{0}$ and $\mathbf{v} = \mathbf{0}$, then $\lim_{\alpha \rightarrow \infty} \mathcal{D}(\tilde{z}, \tilde{\omega}, \tilde{h}, \mathbf{u}, \mathbf{0}, \mathbf{w}) = \mathcal{D}_0(\tilde{z}, \tilde{\omega}, \tilde{h}, \mathbf{w})$.

(v) If $\mathbf{u} = \mathbf{0}$ and $\mathbf{v} = \mathbf{0}$, then

$$\begin{aligned} \lim_{\alpha \rightarrow \infty} \mathcal{D}(\tilde{z}, \tilde{\omega}, \tilde{h}, \mathbf{0}, \mathbf{0}, \mathbf{w}) &= 2\mathcal{D}_0(\tilde{z}, \tilde{\omega}, \tilde{h}, \mathbf{w}) \\ &\quad - \int_0^{\tilde{z}} \tilde{\omega}^2 \hat{\mathcal{B}}_{2\tilde{\omega}}(\tilde{z}', \mathbf{w}) e^{-2i\tilde{h}\tilde{\tau}_0(\tilde{z}')} e^{\bar{G}\bar{G}_0(\tilde{z}')} e^{-2\beta\tilde{\omega}^2 \int_{\tilde{z}'}^{\tilde{z}} \tilde{\mathcal{B}}_0(\tilde{z}'', \mathbf{0}) d\tilde{z}''} d\tilde{z}'. \end{aligned}$$

By comparing the second and third items (or the fourth and fifth items) a sharp transition is noticed from the case $\mathbf{u} = \mathbf{0}$ to $\mathbf{u} \neq \mathbf{0}$. This transition can be studied in detail by looking at small \mathbf{u} of order α^{-1} .

Lemma D.2 (i) If $\mathbf{v} \neq \mathbf{0}$, then $\lim_{\alpha \rightarrow \infty} \mathcal{D}(\tilde{z}, \tilde{\omega}, \tilde{h}, \alpha^{-1}\mathbf{s}, \mathbf{v}, \mathbf{w}) = \mathcal{D}_s(\tilde{z}, \tilde{\omega}, \tilde{h}, \mathbf{v}, \mathbf{w})$ where \mathcal{D}_s is solution of

$$\begin{aligned} \frac{d\mathcal{D}_s}{d\tilde{z}} &= \tilde{\omega}^2 \hat{\mathcal{B}}_{2\tilde{\omega}}(\tilde{z}, \mathbf{w}) e^{-2i\tilde{h}\tilde{\tau}_0(\tilde{z})} e^{\bar{G}\bar{G}_0(\tilde{z})} e^{i\mathbf{s} \cdot \mathbf{v} \frac{\tilde{J}_0(\tilde{z})}{\tilde{\omega}}} + \frac{\beta\tilde{\omega}^2}{(2\pi)^d} \int \hat{\mathcal{B}}_0(\tilde{z}, \boldsymbol{\mu}) \\ &\quad \times \left[e^{i\mathbf{s} \cdot \boldsymbol{\mu} \frac{\tilde{J}_0(\tilde{z})}{\tilde{\omega}}} \mathcal{D}_s(\mathbf{v} - \boldsymbol{\mu}, \mathbf{w} + \boldsymbol{\mu}) + e^{-i\mathbf{s} \cdot \boldsymbol{\mu} \frac{\tilde{J}_0(\tilde{z})}{\tilde{\omega}}} \mathcal{D}_s(\mathbf{v} + \boldsymbol{\mu}, \mathbf{w} + \boldsymbol{\mu}) - 2\mathcal{D}_s(\mathbf{v}, \mathbf{w}) \right] d\boldsymbol{\mu}, \quad (74) \end{aligned}$$

starting from $\mathcal{D}_s(\tilde{z} = 0, \tilde{\omega}, \tilde{h}, \mathbf{v}, \mathbf{w}) = 0$.

(ii) For any \mathbf{s}, \mathbf{s}' , we have

$$\begin{aligned} \lim_{\alpha \rightarrow \infty} \mathcal{D}(\tilde{z}, \tilde{\omega}, \tilde{h}, \alpha^{-1} \mathbf{s}, \alpha^{-1} \mathbf{s}', \mathbf{w}) &= \mathcal{D}_{\mathbf{s}}(\tilde{z}, \tilde{\omega}, \tilde{h}, \mathbf{0}, \mathbf{w}) + \mathcal{D}_{\mathbf{s}'}(\tilde{z}, \tilde{\omega}, \tilde{h}, \mathbf{0}, \mathbf{w}) \\ &\quad - \int_0^{\tilde{z}} \tilde{\omega}^2 \hat{\mathcal{B}}_{2\tilde{\omega}}(\tilde{z}', \mathbf{w}) e^{-2i\tilde{h}\tilde{\tau}_0(\tilde{z}')} e^{\tilde{G}\tilde{G}_0(\tilde{z}')} e^{-2\beta\tilde{\omega}^2 \int_{\tilde{z}'}^{\tilde{z}} \check{\mathcal{B}}_0(\tilde{z}'', \mathbf{0}) d\tilde{z}''} d\tilde{z}'. \end{aligned}$$

By solving the differential equation (74) we obtain the following integral representation of $\mathcal{D}_{\mathbf{s}}(\tilde{z}, \mathbf{v}, \mathbf{w})$ valid for all $\mathbf{s} \in \mathbb{R}^d$:

$$\begin{aligned} \mathcal{D}_{\mathbf{s}}(\tilde{z}, \tilde{\omega}, \tilde{h}, \mathbf{v}, \mathbf{w}) &= \int \int_0^{\tilde{z}} \tilde{\omega}^2 \check{\mathcal{B}}_{2\tilde{\omega}}(\tilde{z}', \boldsymbol{\lambda}) e^{-2i\tilde{h}\tilde{\tau}_0(\tilde{z}')} e^{\tilde{G}\tilde{G}_0(\tilde{z}')} e^{-i\mathbf{w} \cdot \boldsymbol{\lambda}} e^{i\mathbf{v} \cdot \mathbf{s} \frac{\tilde{J}_0(\tilde{z}')}{\tilde{\omega}}} \\ &\quad \times e^{\beta\tilde{\omega}^2 \int_{\tilde{z}'}^{\tilde{z}} \check{\mathcal{B}}_0(\tilde{z}'', \boldsymbol{\lambda} - \frac{\mathbf{s}}{\tilde{\omega}} [\tilde{J}_0(\tilde{z}'') - \tilde{J}_0(\tilde{z}')] + \check{\mathcal{B}}_0(\tilde{z}'', \boldsymbol{\lambda} + \frac{\mathbf{s}}{\tilde{\omega}} [\tilde{J}_0(\tilde{z}'') - \tilde{J}_0(\tilde{z}')] - 2\check{\mathcal{B}}_0(\tilde{z}'', \mathbf{0})) d\tilde{z}''} d\tilde{z}' d\boldsymbol{\lambda}. \end{aligned} \quad (75)$$

In the particular case in which $\mathbf{s} = \mathbf{0}$ the function $\mathcal{D}_{\mathbf{s}}$ is independent of \mathbf{v} and we have

$$\begin{aligned} \lim_{\mathbf{s} \rightarrow \mathbf{0}} \mathcal{D}_{\mathbf{s}}(\tilde{z}, \tilde{\omega}, \tilde{h}, \mathbf{v}, \mathbf{w}) &= \mathcal{D}_{\mathbf{0}}(\tilde{z}, \tilde{\omega}, \tilde{h}, \mathbf{w}) \\ &= \int \int_0^{\tilde{z}} \tilde{\omega}^2 \check{\mathcal{B}}_{2\tilde{\omega}}(\tilde{z}', \boldsymbol{\lambda}) e^{-2i\tilde{h}\tilde{\tau}_0(\tilde{z}')} e^{\tilde{G}\tilde{G}_0(\tilde{z}')} e^{-i\mathbf{w} \cdot \boldsymbol{\lambda}} e^{2\beta\tilde{\omega}^2 \int_{\tilde{z}'}^{\tilde{z}} \check{\mathcal{B}}_0(\tilde{z}'', \boldsymbol{\lambda}) - \check{\mathcal{B}}_0(\tilde{z}'', \mathbf{0}) d\tilde{z}''} d\tilde{z}' d\boldsymbol{\lambda}. \end{aligned}$$

Moreover, we have that

$$\lim_{|\mathbf{s}| \rightarrow \infty} \mathcal{D}_{\mathbf{s}}(\tilde{z}, \tilde{\omega}, \tilde{h}, \mathbf{0}, \mathbf{w}) = \int_0^{\tilde{z}} \tilde{\omega}^2 \hat{\mathcal{B}}_{2\tilde{\omega}}(\tilde{z}', \mathbf{w}) e^{-2i\tilde{h}\tilde{\tau}_0(\tilde{z}')} e^{\tilde{G}\tilde{G}_0(\tilde{z}')} e^{-2\beta\tilde{\omega}^2 \int_{\tilde{z}'}^{\tilde{z}} \check{\mathcal{B}}_0(\tilde{z}'', \mathbf{0}) d\tilde{z}''} d\tilde{z}'.$$

E. Proof of Proposition 4.1

The beam width $R^\varepsilon(t)$ converges to $R(t)$ as $\varepsilon \rightarrow 0$, where $R(t)$ is given by

$$\begin{aligned} R^2(t) &= - \frac{\int \cdots \int \Delta_{\boldsymbol{\kappa}_3} W_{(\boldsymbol{\kappa}_1, \boldsymbol{\kappa}_2), (\boldsymbol{\kappa}_3, \boldsymbol{\kappa}_4)}(\omega, t, L) \overline{\hat{b}_{\text{inc}}(\omega, \boldsymbol{\kappa}_2)} \hat{b}_{\text{inc}}(\omega, \boldsymbol{\kappa}_4) d\boldsymbol{\kappa}_1 d\boldsymbol{\kappa}_2 d\boldsymbol{\kappa}_4 d\omega}{\int \cdots \int W_{(\boldsymbol{\kappa}_1, \boldsymbol{\kappa}_2), (\boldsymbol{\kappa}_1, \boldsymbol{\kappa}_4)}(\omega, t, L) \hat{b}_{\text{inc}}(\omega, \boldsymbol{\kappa}_2) \overline{\hat{b}_{\text{inc}}(\omega, \boldsymbol{\kappa}_4)} d\boldsymbol{\kappa}_1 d\boldsymbol{\kappa}_2 d\boldsymbol{\kappa}_4 d\omega} \\ &= \frac{\int \cdots \int D(\omega, h, L, \mathbf{0}, \boldsymbol{\kappa} + 2\boldsymbol{\kappa}', \boldsymbol{\kappa}) e^{-iht} |\nabla_{\boldsymbol{\kappa}'} \hat{b}_{\text{inc}}(\omega, \boldsymbol{\kappa}')|^2 d\boldsymbol{\kappa} d\boldsymbol{\kappa}' dh d\omega}{\int \cdots \int D(\omega, h, L, \mathbf{0}, \boldsymbol{\kappa} + 2\boldsymbol{\kappa}', \boldsymbol{\kappa}) e^{-iht} |\hat{b}_{\text{inc}}(\omega, \boldsymbol{\kappa}')|^2 d\boldsymbol{\kappa} d\boldsymbol{\kappa}' dh d\omega} \\ &\quad - \frac{\int \cdots \int (\Delta_{\boldsymbol{\kappa}_u} + \Delta_{\boldsymbol{\kappa}_v}) D(\omega, h, L, \mathbf{0}, \boldsymbol{\kappa} + 2\boldsymbol{\kappa}', \boldsymbol{\kappa}) e^{-iht} |\hat{b}_{\text{inc}}(\omega, \boldsymbol{\kappa}')|^2 d\boldsymbol{\kappa} d\boldsymbol{\kappa}' dh d\omega}{\int \cdots \int D(\omega, h, L, \mathbf{0}, \boldsymbol{\kappa} + 2\boldsymbol{\kappa}', \boldsymbol{\kappa}) e^{-iht} |\hat{b}_{\text{inc}}(\omega, \boldsymbol{\kappa}')|^2 d\boldsymbol{\kappa} d\boldsymbol{\kappa}' dh d\omega} \\ &\quad + \frac{\int \cdots \int 2i \nabla_{\boldsymbol{\kappa}_u} D(\omega, h, L, \mathbf{0}, \boldsymbol{\kappa} + 2\boldsymbol{\kappa}', \boldsymbol{\kappa}) e^{-iht} \text{Im}(\overline{\hat{b}_{\text{inc}}(\omega, \boldsymbol{\kappa}')}) \nabla_{\boldsymbol{\kappa}'} \hat{b}_{\text{inc}}(\omega, \boldsymbol{\kappa}') d\boldsymbol{\kappa} d\boldsymbol{\kappa}' dh d\omega}{\int \cdots \int D(\omega, h, L, \mathbf{0}, \boldsymbol{\kappa} + 2\boldsymbol{\kappa}', \boldsymbol{\kappa}) e^{-iht} |\hat{b}_{\text{inc}}(\omega, \boldsymbol{\kappa}')|^2 d\boldsymbol{\kappa} d\boldsymbol{\kappa}' dh d\omega}, \end{aligned} \quad (76)$$

and $D(\omega, h, z, \boldsymbol{\kappa}_u, \boldsymbol{\kappa}_v, \boldsymbol{\kappa}_w)$ is defined by (65). By the identity (66) we have

$$(\Delta_{\boldsymbol{\kappa}_u} + \Delta_{\boldsymbol{\kappa}_v}) D(\omega, h, z, \mathbf{0}, \boldsymbol{\kappa} + 2\boldsymbol{\kappa}', \boldsymbol{\kappa}) = \bar{D} l_x \mathcal{F}_1 \left(\frac{\omega}{\omega_0}, \frac{hL}{\bar{c}}, \frac{z}{L}, (\boldsymbol{\kappa} + 2\boldsymbol{\kappa}') l_x, \boldsymbol{\kappa} l_x \right) e^{2i \frac{hL}{\bar{c}} \tilde{\tau}_0(\frac{z}{L}) - \bar{G}\tilde{G}_0(\frac{z}{L})},$$

$$2\nabla_{\boldsymbol{\kappa}_u} D(\omega, h, z, \mathbf{0}, \boldsymbol{\kappa} + 2\boldsymbol{\kappa}', \boldsymbol{\kappa}) = \bar{D} l_x \mathcal{F}_2 \left(\frac{\omega}{\omega_0}, \frac{hL}{\bar{c}}, \frac{z}{L}, (\boldsymbol{\kappa} + 2\boldsymbol{\kappa}') l_x, \boldsymbol{\kappa} l_x \right) e^{2i \frac{hL}{\bar{c}} \tilde{\tau}_0(\frac{z}{L}) - \bar{G}\tilde{G}_0(\frac{z}{L})},$$

with

$$\mathcal{F}_1(\tilde{\omega}, \tilde{h}, \tilde{z}, \mathbf{v}, \mathbf{w}) = \left[\Delta_{\mathbf{u}} + \Delta_{\mathbf{v}} - 2i \frac{\alpha}{\tilde{\omega}} \tilde{J}_0(\tilde{z}) \mathbf{v} \cdot \nabla_{\mathbf{u}} - \frac{\alpha^2}{\tilde{\omega}^2} \tilde{J}_0(\tilde{z})^2 |\mathbf{v}|^2 \right] \mathcal{D}(\tilde{\omega}, \tilde{h}, \tilde{z}, \mathbf{u}, \mathbf{v}, \mathbf{w}) \Big|_{\mathbf{u}=\mathbf{0}},$$

$$\mathcal{F}_2(\tilde{\omega}, \tilde{h}, \tilde{z}, \mathbf{v}, \mathbf{w}) = \left[2\nabla_{\mathbf{u}} - 2 \frac{\alpha}{\tilde{\omega}} i \tilde{J}_0(\tilde{z}) \mathbf{v} \right] \mathcal{D}(\tilde{\omega}, \tilde{h}, \tilde{z}, \mathbf{u}, \mathbf{v}, \mathbf{w}) \Big|_{\mathbf{u}=\mathbf{0}}.$$

In the limit $\alpha \rightarrow \infty$, we obtain by using Lemma D.2

$$\begin{aligned} & \frac{e^{-2i\frac{hL}{c}\tilde{\tau}_0(1)+\bar{G}\bar{G}_0(1)}}{(2\pi)^d\bar{D}\alpha^2} \int (\Delta_{\boldsymbol{\kappa}_1} + \Delta_{\boldsymbol{\kappa}_2}) D(\omega, h, L, \mathbf{0}, \boldsymbol{\kappa} + 2\boldsymbol{\kappa}', \boldsymbol{\kappa}) d\boldsymbol{\kappa} \xrightarrow{\alpha \rightarrow \infty} \\ & \int_0^1 \Delta_\lambda \check{\mathcal{B}}_{2\frac{\omega}{\omega_0}}(\tilde{z}, \mathbf{0}) e^{-2i\frac{hL}{c}\tilde{\tau}_0(\tilde{z})} e^{\bar{G}\bar{G}_0(\tilde{z})} (\tilde{J}_0(1) - \tilde{J}_0(\tilde{z}))^2 d\tilde{z} \\ & - 4|\boldsymbol{\kappa}'|_x^2 l_x^2 \int_0^1 \check{\mathcal{B}}_{2\frac{\omega}{\omega_0}}(\tilde{z}, \mathbf{0}) e^{-2i\frac{hL}{c}\tilde{\tau}_0(\tilde{z})} e^{\bar{G}\bar{G}_0(\tilde{z})} (\tilde{J}_0(1) - \tilde{J}_0(\tilde{z}))^2 d\tilde{z} \\ & + 2\beta \int_0^1 \frac{\omega^2}{\omega_0^2} \check{\mathcal{B}}_{2\frac{\omega}{\omega_0}}(\tilde{z}, \mathbf{0}) e^{-2i\frac{hL}{c}\tilde{\tau}_0(\tilde{z})} e^{\bar{G}\bar{G}_0(\tilde{z})} \\ & \quad \times \int_{\tilde{z}}^1 \Delta_\lambda \check{\mathcal{B}}_0(\tilde{z}', \mathbf{0}) [(\tilde{J}_0(1) - \tilde{J}_0(\tilde{z}))^2 + (\tilde{J}_0(\tilde{z}) - \tilde{J}_0(\tilde{z}'))^2] d\tilde{z}' d\tilde{z}, \end{aligned}$$

and

$$\begin{aligned} & \frac{e^{-2i\frac{hL}{c}\tilde{\tau}_0(1)+\bar{G}\bar{G}_0(1)}}{(2\pi)^d\bar{D}\alpha} \int 2\nabla_{\boldsymbol{\kappa}_1} D(\omega, h, L, \mathbf{0}, \boldsymbol{\kappa} + 2\boldsymbol{\kappa}', \boldsymbol{\kappa}) d\boldsymbol{\kappa} \xrightarrow{\alpha \rightarrow \infty} \\ & - 4i\boldsymbol{\kappa}' l_x \int_0^1 \frac{\omega}{\omega_0} \check{\mathcal{B}}_{2\frac{\omega}{\omega_0}}(\tilde{z}, \mathbf{0}) e^{-2i\frac{hL}{c}\tilde{\tau}_0(\tilde{z})} e^{\bar{G}\bar{G}_0(\tilde{z})} (\tilde{J}_0(1) - \tilde{J}_0(\tilde{z})) d\tilde{z}. \end{aligned}$$

Substituting these limits into (76) we obtain that, in the large- α regime, the beam radius is

$$\begin{aligned} R^2(t) &= R_0^2 - 2\beta\alpha^2 l_x^2 \int_{\tilde{z}(t)}^1 \Delta_\lambda \check{\mathcal{B}}_0(\tilde{z}', \mathbf{0}) [(\tilde{J}_0(1) - \tilde{J}_0(\tilde{z}(t)))^2 + (\tilde{J}_0(\tilde{z}(t)) - \tilde{J}_0(\tilde{z}'))^2] d\tilde{z}' \\ & + 4\alpha^2 l_x^4 \frac{\int \check{\mathcal{B}}_{2\frac{\omega}{\omega_0}}(\tilde{z}(t), \mathbf{0}) \int |\boldsymbol{\kappa}'|^2 |\hat{b}_{\text{inc}}(\omega, \boldsymbol{\kappa}')|^2 d\boldsymbol{\kappa}' d\omega}{\int \frac{\omega^2}{\omega_0^2} \check{\mathcal{B}}_{2\frac{\omega}{\omega_0}}(\tilde{z}(t), \mathbf{0}) \int |\hat{b}_{\text{inc}}(\omega, \boldsymbol{\kappa}')|^2 d\boldsymbol{\kappa}' d\omega} (\tilde{J}_0(1) - \tilde{J}_0(\tilde{z}(t)))^2 \\ & + 4\alpha^2 l_x^2 \frac{\int \frac{\omega}{\omega_0} \check{\mathcal{B}}_{2\frac{\omega}{\omega_0}}(\tilde{z}(t), \mathbf{0}) \int \boldsymbol{\kappa} \cdot \text{Im}(\hat{b}_{\text{inc}} \overline{\nabla_{\boldsymbol{\kappa}} \hat{b}_{\text{inc}}(\omega, \boldsymbol{\kappa})}) d\boldsymbol{\kappa}' d\omega}{\int \frac{\omega^2}{\omega_0^2} \check{\mathcal{B}}_{2\frac{\omega}{\omega_0}}(\tilde{z}(t), \mathbf{0}) \int |\hat{b}_{\text{inc}}(\omega, \boldsymbol{\kappa}')|^2 d\boldsymbol{\kappa}' d\omega} (\tilde{J}_0(1) - \tilde{J}_0(\tilde{z}(t))) \\ & - \alpha^2 l_x^2 \frac{\int \Delta_\lambda \check{\mathcal{B}}_{2\frac{\omega}{\omega_0}}(\tilde{z}(t), \mathbf{0}) \int |\hat{b}_{\text{inc}}(\omega, \boldsymbol{\kappa}')|^2 d\boldsymbol{\kappa}' d\omega}{\int \frac{\omega^2}{\omega_0^2} \check{\mathcal{B}}_{2\frac{\omega}{\omega_0}}(\tilde{z}(t), \mathbf{0}) \int |\hat{b}_{\text{inc}}(\omega, \boldsymbol{\kappa}')|^2 d\boldsymbol{\kappa}' d\omega} (\tilde{J}_0(1) - \tilde{J}_0(\tilde{z}(t)))^2, \end{aligned}$$

where $\tilde{z}(t)$ is defined by (71). If we assume that the relative bandwidth $B \ll 1$ so that $\check{\mathcal{B}}_{2\tilde{\omega}}(\tilde{z}, \boldsymbol{\lambda}) \simeq \check{\mathcal{B}}_2(\tilde{z}, \boldsymbol{\lambda})$ for any $\tilde{\omega} \in (1 - B, 1 + B)$, then the expression can be simplified into

$$\begin{aligned} R^2(t) &= R_0^2 - 2\beta\alpha^2 l_x^2 \int_{\tilde{z}(t)}^1 \Delta_\lambda \check{\mathcal{B}}_0(\tilde{z}', \mathbf{0}) [(\tilde{J}_0(1) - \tilde{J}_0(\tilde{z}(t)))^2 + (\tilde{J}_0(\tilde{z}') - \tilde{J}_0(\tilde{z}(t)))^2] d\tilde{z}' \\ & + 4K_0^2 l_x^4 \alpha^2 (\tilde{J}_0(1) - \tilde{J}_0(\tilde{z}(t)))^2 + 4Q_0 l_x^2 \alpha (\tilde{J}_0(1) - \tilde{J}_0(\tilde{z}(t))) \\ & - \alpha^2 l_x^2 \frac{\Delta_\lambda \check{\mathcal{B}}_2(\tilde{z}(t), \mathbf{0})}{\check{\mathcal{B}}_2(\tilde{z}(t), \mathbf{0})} (\tilde{J}_0(1) - \tilde{J}_0(\tilde{z}(t)))^2. \end{aligned}$$

We can write $R(t)$ in terms of the original variables by using the expressions (33) of α and β , which gives (35).

F. Proof of Proposition 4.2

The spectral width $K^\varepsilon(t)$ converges to $K(t)$ as $\varepsilon \rightarrow 0$, where $K(t)$ is given by

$$\begin{aligned} K^2(t) &= \frac{\int \cdots \int |\boldsymbol{\kappa}_1|^2 W_{(\boldsymbol{\kappa}_1, \boldsymbol{\kappa}_2), (\boldsymbol{\kappa}_1, \boldsymbol{\kappa}_4)}(\omega, t, L) \hat{b}_{\text{inc}}(\omega, \boldsymbol{\kappa}_2) \overline{\hat{b}_{\text{inc}}(\omega, \boldsymbol{\kappa}_4)} d\boldsymbol{\kappa}_1 d\boldsymbol{\kappa}_2 d\boldsymbol{\kappa}_4 d\omega}{\int \cdots \int W_{(\boldsymbol{\kappa}_1, \boldsymbol{\kappa}_2), (\boldsymbol{\kappa}_1, \boldsymbol{\kappa}_4)}(\omega, t, L) \hat{b}_{\text{inc}}(\omega, \boldsymbol{\kappa}_2) \overline{\hat{b}_{\text{inc}}(\omega, \boldsymbol{\kappa}_4)} d\boldsymbol{\kappa}_1 d\boldsymbol{\kappa}_2 d\boldsymbol{\kappa}_4 d\omega} \\ &= \frac{\int \cdots \int |\boldsymbol{\kappa} + \boldsymbol{\kappa}'|^2 D(\omega, h, L, \mathbf{0}, \boldsymbol{\kappa} + 2\boldsymbol{\kappa}', \boldsymbol{\kappa}) e^{-iht} |\hat{b}_{\text{inc}}(\omega, \boldsymbol{\kappa}')|^2 d\boldsymbol{\kappa} d\boldsymbol{\kappa}' dh d\omega}{\int \cdots \int D(\omega, h, L, \mathbf{0}, \boldsymbol{\kappa} + 2\boldsymbol{\kappa}', \boldsymbol{\kappa}) |\hat{b}_{\text{inc}}(\omega, \boldsymbol{\kappa}')|^2 e^{-iht} d\boldsymbol{\kappa} d\boldsymbol{\kappa}' dh d\omega}. \end{aligned} \quad (77)$$

In the limit $\alpha \rightarrow \infty$ we obtain

$$K^2(t) = K_0^2 - 2\beta l_x^{-2} \int_{\tilde{z}(t)}^1 \Delta_\lambda \check{\mathcal{B}}_0(\tilde{z}', \mathbf{0}) d\tilde{z}' - \frac{\Delta_\lambda \check{\mathcal{B}}_2(\tilde{z}(t), \mathbf{0})}{\check{\mathcal{B}}_2(\tilde{z}(t), \mathbf{0})} l_x^{-2}, \quad (78)$$

where K_0 is the spectral width (36) of the incoming beam. Substituting the value of β we get the expression (41).

G. Proof of Proposition 4.3

The spatial cross correlation function $A^\varepsilon(t, \mathbf{x})$ has the limit $A(t, \mathbf{x})$ as $\varepsilon \rightarrow 0$:

$$\begin{aligned} A(t, \mathbf{x}) &= \frac{\int \cdots \int W_{(\boldsymbol{\kappa}_1, \boldsymbol{\kappa}_2), (\boldsymbol{\kappa}_1, \boldsymbol{\kappa}_4)}(\omega, t, L) e^{-i(\boldsymbol{\kappa}_1 - \boldsymbol{\kappa}_2 + \boldsymbol{\kappa}_4) \cdot \mathbf{x}} \hat{b}_{\text{inc}}(\omega, \boldsymbol{\kappa}_2) \overline{\hat{b}_{\text{inc}}(\omega, \boldsymbol{\kappa}_4)} d\boldsymbol{\kappa}_1 d\boldsymbol{\kappa}_2 d\boldsymbol{\kappa}_4 d\omega}{\int \cdots \int W_{(\boldsymbol{\kappa}_1, \boldsymbol{\kappa}_2), (\boldsymbol{\kappa}_1, \boldsymbol{\kappa}_4)}(\omega, t, L) \hat{b}_{\text{inc}}(\omega, \boldsymbol{\kappa}_2) \overline{\hat{b}_{\text{inc}}(\omega, \boldsymbol{\kappa}_4)} d\boldsymbol{\kappa}_1 d\boldsymbol{\kappa}_2 d\boldsymbol{\kappa}_4 d\omega} \\ &= \frac{\int \cdots \int D(\omega, h, L, \mathbf{0}, \boldsymbol{\kappa} + \boldsymbol{\kappa}', \boldsymbol{\kappa} - \boldsymbol{\kappa}') e^{-iht} e^{-i\boldsymbol{\kappa} \cdot \mathbf{x}} |\hat{b}_{\text{inc}}(\omega, \boldsymbol{\kappa}')|^2 d\boldsymbol{\kappa} d\boldsymbol{\kappa}' dh d\omega}{\int \cdots \int D(\omega, h, L, \mathbf{0}, \boldsymbol{\kappa} + 2\boldsymbol{\kappa}', \boldsymbol{\kappa}) e^{-iht} |\hat{b}_{\text{inc}}(\omega, \boldsymbol{\kappa}')|^2 d\boldsymbol{\kappa} d\boldsymbol{\kappa}' dh d\omega}. \end{aligned}$$

In the limit $\alpha \rightarrow \infty$, we obtain by using Lemma D.1 that $A(t, \mathbf{x})$ has the form:

$$A(t, \mathbf{x}) = \frac{\int \frac{\omega^2}{\omega_0^2} \check{\mathcal{B}}_{2\frac{\omega}{\omega_0}}(\tilde{z}(t), \frac{\mathbf{x}}{l_x}) e^{2\beta \frac{\omega^2}{\omega_0^2} \int_{\tilde{z}(t)}^1 \check{\mathcal{B}}_0(\tilde{z}', \frac{\mathbf{x}}{l_x}) - \check{\mathcal{B}}_0(\tilde{z}', \mathbf{0}) d\tilde{z}'} \left[\int e^{-i\boldsymbol{\kappa}' \cdot \mathbf{x}} |\hat{b}_{\text{inc}}(\omega, \boldsymbol{\kappa}')|^2 d\boldsymbol{\kappa}' \right] d\omega}{\int \frac{\omega^2}{\omega_0^2} \check{\mathcal{B}}_{2\frac{\omega}{\omega_0}}(\tilde{z}(t), \mathbf{0}) \left[\int |\hat{b}_{\text{inc}}(\omega, \boldsymbol{\kappa}')|^2 d\boldsymbol{\kappa}' \right] d\omega},$$

where $\tilde{z}(t)$ is defined by (71). If we assume that the relative bandwidth $B \ll 1$ so that $\check{\mathcal{B}}_{2\tilde{\omega}}(\tilde{z}, \boldsymbol{\lambda}) \simeq \check{\mathcal{B}}_2(\tilde{z}, \boldsymbol{\lambda})$ for any $\tilde{\omega} \in (1 - B, 1 + B)$, then the expression can be simplified to

$$A(t, \mathbf{x}) = \frac{\check{\mathcal{B}}_2(\tilde{z}(t), \frac{\mathbf{x}}{l_x})}{\check{\mathcal{B}}_2(\tilde{z}(t), \mathbf{0})} e^{2\beta \int_{\tilde{z}(t)}^1 \check{\mathcal{B}}_0(\tilde{z}', \frac{\mathbf{x}}{l_x}) - \check{\mathcal{B}}_0(\tilde{z}', \mathbf{0}) d\tilde{z}'} \frac{\iint e^{-i\boldsymbol{\kappa}' \cdot \mathbf{x}} |\hat{b}_{\text{inc}}(\omega, \boldsymbol{\kappa}')|^2 d\boldsymbol{\kappa}' d\omega}{\iint |\hat{b}_{\text{inc}}(\omega, \boldsymbol{\kappa}')|^2 d\boldsymbol{\kappa}' d\omega}.$$

In the original variables, we obtain (43).

H. Proof of Proposition 4.4

The spectral cross correlation function $S^\varepsilon(t, \boldsymbol{\kappa})$ has the limit $S(t, \boldsymbol{\kappa})$ as $\varepsilon \rightarrow 0$:

$$\begin{aligned} S(t, \boldsymbol{\kappa}) &= \frac{\int \cdots \int W_{(\boldsymbol{\kappa}_1, \boldsymbol{\kappa}_2), (\boldsymbol{\kappa}_1 + \boldsymbol{\kappa}, \boldsymbol{\kappa}_4)}(\omega, t, L) \hat{b}_{\text{inc}}(\omega, \boldsymbol{\kappa}_2) \overline{\hat{b}_{\text{inc}}(\omega, \boldsymbol{\kappa}_4)} d\boldsymbol{\kappa}_1 d\boldsymbol{\kappa}_2 d\boldsymbol{\kappa}_4 d\omega}{\int \cdots \int W_{(\boldsymbol{\kappa}_1, \boldsymbol{\kappa}_2), (\boldsymbol{\kappa}_1, \boldsymbol{\kappa}_4)}(\omega, t, L) \hat{b}_{\text{inc}}(\omega, \boldsymbol{\kappa}_2) \overline{\hat{b}_{\text{inc}}(\omega, \boldsymbol{\kappa}_4)} d\boldsymbol{\kappa}_1 d\boldsymbol{\kappa}_2 d\boldsymbol{\kappa}_4 d\omega} \\ &= \frac{\int \cdots \int D(\omega, h, L, -\boldsymbol{\kappa}, \boldsymbol{\kappa}_1 + \boldsymbol{\kappa}_2 + \boldsymbol{\kappa}, \boldsymbol{\kappa}_1 - \boldsymbol{\kappa}_2) e^{-iht} \hat{b}_{\text{inc}}(\omega, \boldsymbol{\kappa}_2) \overline{\hat{b}_{\text{inc}}(\omega, \boldsymbol{\kappa}_2 + \boldsymbol{\kappa})} d\boldsymbol{\kappa}_1 d\boldsymbol{\kappa}_2 dh d\omega}{\int \cdots \int D(\omega, h, L, \mathbf{0}, \boldsymbol{\kappa}_1 + \boldsymbol{\kappa}_2, \boldsymbol{\kappa}_1 - \boldsymbol{\kappa}_2) e^{-iht} |\hat{b}_{\text{inc}}(\omega, \boldsymbol{\kappa}_2)|^2 d\boldsymbol{\kappa}_1 d\boldsymbol{\kappa}_2 dh d\omega}. \end{aligned}$$

In the limit $\alpha \rightarrow \infty$, we obtain by using Lemma D.1 that $S(t, \alpha^{-1}\boldsymbol{\kappa})$ has the form:

$$S(t, \alpha^{-1}\boldsymbol{\kappa}) = \frac{\iint \frac{\omega^2}{\omega_0^2} \check{\mathcal{B}}_{2\frac{\omega}{\omega_0}} \left(\tilde{z}(t), \frac{\omega_0}{\omega} (\tilde{J}_0(1) - \tilde{J}_0(\tilde{z}(t))) \boldsymbol{\kappa} l_x \right) |\hat{b}_{\text{inc}}(\omega, \boldsymbol{\kappa}_2)|^2 X(\omega, \boldsymbol{\kappa}_2) d\boldsymbol{\kappa}_2 d\omega}{\iint \frac{\omega^2}{\omega_0^2} \check{\mathcal{B}}_{2\frac{\omega}{\omega_0}} (\tilde{z}(t), \mathbf{0}) |\hat{b}_{\text{inc}}(\omega, \boldsymbol{\kappa}_2)|^2 d\boldsymbol{\kappa}_2 d\omega},$$

$$X(\omega, \boldsymbol{\kappa}_2) = e^{\beta \frac{\omega^2}{\omega_0^2} \int_{\tilde{z}(t)}^1 \check{\mathcal{B}}_0(\tilde{z}', \boldsymbol{\kappa} l_x \frac{\omega}{\omega_0} [\tilde{J}_0(1) - 2\tilde{J}_0(\tilde{z}(t)) + \tilde{J}_0(\tilde{z}')] + \check{\mathcal{B}}_0(\tilde{z}', \boldsymbol{\kappa} l_x \frac{\omega}{\omega_0} [\tilde{J}_0(1) - \tilde{J}_0(\tilde{z}')] - 2\check{\mathcal{B}}_0(\tilde{z}', \mathbf{0}) d\tilde{z}'}$$

$$\times e^{2i \frac{\omega_0}{\omega} (\tilde{J}_0(1) - \tilde{J}_0(\tilde{z}(t))) \boldsymbol{\kappa} \cdot \boldsymbol{\kappa}_2 l_x^2},$$

where $\tilde{z}(t)$ is defined by (71). If we assume that the relative bandwidth $B \ll 1$ so that $\check{\mathcal{B}}_{2\tilde{\omega}}(\tilde{z}, \boldsymbol{\lambda}) \simeq \check{\mathcal{B}}_2(\tilde{z}, \boldsymbol{\lambda})$ for any $\tilde{\omega} \in (1 - B, 1 + B)$, then the expression can be simplified to

$$S(t, \alpha^{-1}\boldsymbol{\kappa}) = \frac{\check{\mathcal{B}}_2 \left(\tilde{z}(t), (\tilde{J}_0(1) - \tilde{J}_0(\tilde{z}(t))) \boldsymbol{\kappa} l_x \right)}{\check{\mathcal{B}}_2(\tilde{z}(t), \mathbf{0})}$$

$$\times e^{\beta \int_{\tilde{z}(t)}^1 \check{\mathcal{B}}_0(\tilde{z}', \boldsymbol{\kappa} l_x [\tilde{J}_0(1) - 2\tilde{J}_0(\tilde{z}(t)) + \tilde{J}_0(\tilde{z}')] + \check{\mathcal{B}}_0(\tilde{z}', \boldsymbol{\kappa} l_x [\tilde{J}_0(1) - \tilde{J}_0(\tilde{z}')] - 2\check{\mathcal{B}}_0(\tilde{z}', \mathbf{0}) d\tilde{z}'}$$

$$\times \frac{\iint e^{2i(\tilde{J}_0(1) - \tilde{J}_0(\tilde{z}(t))) \boldsymbol{\kappa} \cdot \boldsymbol{\kappa}_2 l_x^2} |\hat{b}_{\text{inc}}(\omega, \boldsymbol{\kappa}_2)|^2 d\boldsymbol{\kappa}_2 d\omega}{\iint |\hat{b}_{\text{inc}}(\omega, \boldsymbol{\kappa}')|^2 d\boldsymbol{\kappa}' d\omega}.$$

In the original variables, we obtain (44).

I. Proof of Proposition 4.5

The mean reflected power observed in the relative direction $\boldsymbol{\kappa}$ is given by

$$P_{\boldsymbol{\kappa}}(t) = \frac{1}{(2\pi)^{d+1}} \int \cdots \int W_{(-\boldsymbol{\kappa}_0 + \boldsymbol{\kappa}, \boldsymbol{\kappa}_2), (-\boldsymbol{\kappa}_0 + \boldsymbol{\kappa}, \boldsymbol{\kappa}_4)}(\omega, t, L) \hat{b}_{\text{inc}}(\omega, \boldsymbol{\kappa}_2) \overline{\hat{b}_{\text{inc}}(\omega, \boldsymbol{\kappa}_4)} d\boldsymbol{\kappa}_0 d\boldsymbol{\kappa}_2 d\boldsymbol{\kappa}_4 d\omega$$

$$= \frac{1}{(2\pi)^{d+2}} \int \cdots \int D(\omega, h, L, \mathbf{0}, -\boldsymbol{\kappa}_0 + \boldsymbol{\kappa} + \boldsymbol{\kappa}_2, -\boldsymbol{\kappa}_0 + \boldsymbol{\kappa} - \boldsymbol{\kappa}_2) e^{-iht} |\hat{b}_{\text{inc}}(\omega, \boldsymbol{\kappa}_2)|^2 d\boldsymbol{\kappa}_0 d\boldsymbol{\kappa}_2 dh d\omega.$$

If we take into account the fact that the angular aperture of the input beam is very small, i.e. much smaller than $\alpha^{-1}(\omega_0 l_x / \bar{c})^{-1}$, and that it is quasi-monochromatic, i.e. $B \ll 1$, then we find that the mean reflected power observed in the relative direction $\boldsymbol{\kappa}$ is

$$P_{\boldsymbol{\kappa}}(t) = \frac{E_{\text{inc}}}{2\pi} \iint D(\omega_0, h, L, \mathbf{0}, \boldsymbol{\kappa}, -2\boldsymbol{\kappa}_0 + \boldsymbol{\kappa}) e^{-iht} dh d\boldsymbol{\kappa}_0, \quad (79)$$

where E_{inc} is the input energy defined by (32). In the large- α regime, we observe the reflected wave in a cone of angular aperture of order α^{-1} and by Lemma D.2:

$$P_{\alpha^{-1}\boldsymbol{\kappa}}(t) \xrightarrow{\alpha \rightarrow \infty} \frac{\pi^d E_{\text{inc}} \bar{D} \bar{c} \tilde{c}_0(\tilde{z}(t))}{2L} \check{\mathcal{B}}_2(\tilde{z}(t), \mathbf{0}) e^{\bar{G}[\tilde{G}_0(\tilde{z}(t)) - \tilde{G}_0(1)]}$$

$$\times \left[1 - e^{-2\beta \int_{\tilde{z}(t)}^1 \check{\mathcal{B}}_0(\tilde{z}', \mathbf{0}) d\tilde{z}'} + e^{2\beta \int_{\tilde{z}(t)}^1 \check{\mathcal{B}}_0(\tilde{z}', \boldsymbol{\kappa} l_x [\tilde{J}_0(1) - \tilde{J}_0(\tilde{z}')] - \check{\mathcal{B}}_0(\tilde{z}', \mathbf{0}) d\tilde{z}'} \right],$$

where $\tilde{z}(t)$ is defined by (71). In the original variables we obtain (46).

References

- [1] Asch, M., Kohler, W., Papanicolaou, G., Postel, M., White, B.: Frequency content of randomly scattered signals. *SIAM Rev.* 33, 519-625 (1991)
- [2] Barabanenkov, Y.N: Wave corrections for the transfer equation for backward scattering. *Izv. Vyssh. Uchebn. Zaved. Radiofiz.* 16, 88-96 (1973)
- [3] Claerbout, J.F.: *Imaging the Earth's interior*. Blackwell Scientific Publications, Palo Alto, 1985.
- [4] Fante, R.L.: Wave propagation in random media: a systematic approach. *Progress in Optics*, Wolf, E., ed., (Elsevier, Amsterdam, 1985), Vol. 22, 341-398
- [5] Fouque, J.-P., Garnier, J., Nachbin, A., Sølna, K.: Imaging of a dissipative layer in a random medium using a time reversal method. In: *Monte Carlo and Quasi-Monte Carlo Methods 2004*, Niederreiter, H., Talay, D. (eds.), pp. 127-145, Springer, Berlin (2006)
- [6] Fouque, J.-P., Garnier, J., Papanicolaou, G., Sølna, K.: *Wave propagation and time reversal in randomly layered media*. Springer, New York (2007)
- [7] Fouque, J.-P., Poliannikov, O.: Time reversal detection in one-dimensional random media. *Inverse Problems* 22, 903-922 (2006)
- [8] Garnier, J., Sølna, K.: Random backscattering in the parabolic scaling. *J. Stat. Phys.* 131, 445-486 (2008)
- [9] Huang, K., Papanicolaou, G., Sølna, K., Tsonga, C., Zhao, H.: Efficient numerical simulation for long range wave propagation. *J. Comput. Phys.* 215, 448-464 (2005)
- [10] Labeyrie, G., de Tomasi, F., Bernard, J.-C., Müller, C.A., Miniatura, C., Kaiser, R.: Coherent backscattering of light by atoms. *Phys. Rev. Lett.* 83, 5266-5269 (1999)
- [11] Papanicolaou, G., Postel, M., Sheng, P. White, B.: Frequency content of randomly scattered signals. Part II: Inversion. *Wave Motion* 12, 527-549 (1990)
- [12] Strohbehn, J.W. (ed.): *Laser beam propagation in the atmosphere*. Springer, Berlin (1978)
- [13] Tappert, F.: The parabolic approximation method. In: *Wave propagation and underwater acoustics*, Keller, J.B., Papadakis, J.S. (eds.), pp. 224-287, Springer, Berlin (1977)
- [14] Thrane, L., Yura, H.T., Andersen, P.E.: Analysis of optical coherence tomography systems based on the extended Huygens-Fresnel principle. *J. Opt. Soc. Am. A* 17, 484-490 (2000)
- [15] Tourin, A., Derode, A., Roux, P., van Tiggelen, B.A., Fink, M.: Time-dependent coherent backscattering of acoustic waves. *Phys. Rev. Lett.* 79, 3637-3639 (1997)
- [16] van Albada, M.P., Lagendijk, A.: Observation of weak localization of light in a random medium. *Phys. Rev. Lett.* 55, 2692-2695 (1985)
- [17] van Rossum, M.C.W., Nieuwenhuizen, Th.M.: Multiple scattering of classical waves: microscopy, mesoscopy, and diffusion. *Rev. Mod. Phys.* 71, 313-371 (1999)
- [18] White, B., Sheng, P., Postel, M., Papanicolaou, G.: Probing through cloudiness: Theory of statistical inversion for multiply scattered data. *Phys. Rev. Lett.* 63, 2228-2231 (1989)
- [19] Wolf, P.E., Maret, G.: Weak localization and coherent backscattering of photons in disordered media. *Phys. Rev. Lett.* 55, 2696-2699 (1985)